NASA TECHNICAL
MEMORANDUM

NASA TM X-2076

NASA TM X-2076

COOLANT FLOW EFFECTS ON THE PERFORMANCE OF A CONICAL PLUG NOZZLE AT MACH NUMBERS FROM 0 TO 2.0

by Robert J. Jeracki and Francis C. Chenoweth

Lewis Research Center
Cleveland, Ohio 44135

NATIONAL AERONAUTICS AND SPACE ADMINISTRATION • WASHINGTON, D. C. • SEPTEMBER 1970

1. Report No. NASA TM X-2076	2. Government Accession No.	3. Recipient's Catalog No.
4. Title and Subtitle COOLANT FLOW EFFECTS ON THE PERFORMANCE OF A CONICAL PLUG NOZZLE AT MACH NUMBERS FROM 0 TO 2.0		5. Report Date September 1970 6. Performing Organization Code
7. Author(s) Robert J. Jeracki and Francis C. Chenoweth		8. Performing Organization Report No. E-5552
9. Performing Organization Name and Address Lewis Research Center National Aeronautics and Space Administration Cleveland, Ohio 44135		10. Work Unit No. 720-03 11. Contract or Grant No.
12. Sponsoring Agency Name and Address National Aeronautics and Space Administration Washington, D. C. 20546		13. Type of Report and Period Covered Technical Memorandum 14. Sponsoring Agency Code
15. Supplementary Notes		

16. Abstract

The effect of film cooling on nozzle performance was evaluated for three cooling slot locations on the plug surface: one upstream and two downstream of the nozzle throat. An additional configuration simulated a convectively cooled plug truncated to half-length with the coolant flow dumped into the plug base. The primary throat was maintained in the maximum afterburning position with a throat to nacelle area ratio of 0.36. All configurations had nozzle efficiencies within 1.5 percent of each other at takeoff and at three important acceleration conditions. These configurations typically provided nozzle efficiencies of 99 percent at takeoff, 95 percent at Mach 1.2, and 97 percent at Mach 1.97. The coolant slot upstream of the throat generally provided the highest nozzle efficiency but also required the highest coolant pressures.

17. Key Words (Suggested by Author(s))	18. Distribution Statement
Plug nozzle cooling Cooling flow effects Performance of plug nozzle Film cooling effects	Unclassified - unlimited

19. Security Classif. (of this report)	20. Security Classif. (of this page)	21. No. of Pages	22. Price*
Unclassified	Unclassified	50	$3.00

*For sale by the Clearinghouse for Federal Scientific and Technical Information
Springfield, Virginia 22151

COOLANT FLOW EFFECTS ON THE PERFORMANCE OF A CONICAL PLUG NOZZLE AT MACH NUMBERS FROM 0 to 2.0

by Robert J. Jeracki and Francis C. Chenoweth

Lewis Research Center

SUMMARY

An experimental investigation was conducted in the Lewis 8- by 6-Foot Supersonic Wind Tunnel to determine coolant flow effects on the performance of a low-angle conical plug nozzle designed for a supersonic cruise aircraft. The primary throat area was fixed in the maximum afterburning position with a throat to nacelle area ratio of 0.36. Film coolant slots were evaluated at three locations on the plug surface, one upstream and two downstream of the nozzle throat. An additional configuration simulated a convectively cooled plug truncated to half-length with the coolant flow dumped into the plug base. These configurations were evaluated over a Mach number range from 0 to 1.97 using room temperature air for both the primary and coolant flows.

At takeoff and at three typical acceleration conditions (Mach 0.9, 1.2, and 1.97) all configurations had nozzle efficiencies within 1.5 percent of each other for a corrected coolant flow rate of 2 percent. The coolant slot upstream of the nozzle throat generally provided the highest nozzle efficiency but also required the highest coolant pressures. For a typical turbojet acceleration schedule all cooling configurations provided high nozzle efficiency at Mach numbers from 0 to 1.97. For example, nozzle efficiencies varied from about 99 percent at takeoff to a minimum of 95 percent at Mach 1.2 and then increased to about 97 percent at Mach 1.97.

All coolant slots downstream of the throat generally were choked (except for the truncated plug at subsonic Mach numbers) and required coolant total pressures of about 75 percent of the primary total pressure to provide a corrected coolant flow rate of 2 percent. A slot of similar size located upstream of the throat was not choked for the same coolant flow and required a total pressure about equal to the primary total pressure. This coolant pressure was reduced to about 80 percent of the primary total pressure by increasing the coolant flow area by 70 percent. This increase in slot area resulted in a slight loss in nozzle efficiency.

INTRODUCTION

The Lewis Research Center is evaluating various exhaust nozzle concepts for application to supersonic cruise aircraft. Results from this continuing program (ref. 1) indicate that a low angle conical plug nozzle with a translating external cylindrical shroud can provide high nozzle efficiency over a wide range of flight conditions. This nozzle consists of a rigid plug and varies primary throat area with an iris flap. The plug is immersed in the hot exhaust stream of the afterburning engine. Cooling the plug, therefore, represents a significant problem in that various cooling techniques and their effect on nozzle performance must be optimized. Numerous schemes have been proposed for cooling a surface imbedded in a hot gas (ref. 2). These include convection, film, transpiration, and regenerative cooling techniques. Both liquids and gases are used as the cooling mediums.

The 8.5-inch- (21.6-cm-) diameter plug nozzle of reference 1 was used in the current test program to evaluate the effect of several cooling configurations on nozzle efficiency and coolant pumping characteristics. Dry air at room temperature was used for both the primary and coolant flows. Variations in the coolant flow rate were studied up to a maximum value of 20 percent of the primary flow. The test was conducted in the Lewis Research Center 8- by 6-Foot Supersonic Wind Tunnel at Mach numbers from 0 to 1.97. The external shroud was retracted for Mach numbers from 0 to 1.2 and extended at Mach numbers of 1.2 to 1.97.

APPARATUS AND PROCEDURE

Installation

The nozzles were evaluated on an 8.5-inch jet exit model mounted in the transonic test section of the Lewis 8- by 6-Foot Supersonic Wind Tunnel as shown in figure 1. The grounded portion of the model (fig. 2) was supported from the tunnel ceiling by a thin vertical strut with a 50.25-inch (127.63-cm) chord and a thickness-to-chord ratio of 0.035. This straight strut had leading and trailing edge wedge angles of 10°. Symbols used in this report are defined in appendix A. The model uses a closed nose with an l/d_{max} of 3.0 followed by a cylindrical section back to the nozzle attachment station.

The forebody was composed of a 15° half-angle conical tip which was faired into the cylindrical section with a circular arc whose radius was approximately 8.0 d_{max}. The floating portion of the model, which includes the horizontal primary and secondary (coolant) air bottles and exhaust nozzle, was cantilevered by flow tubes from supply

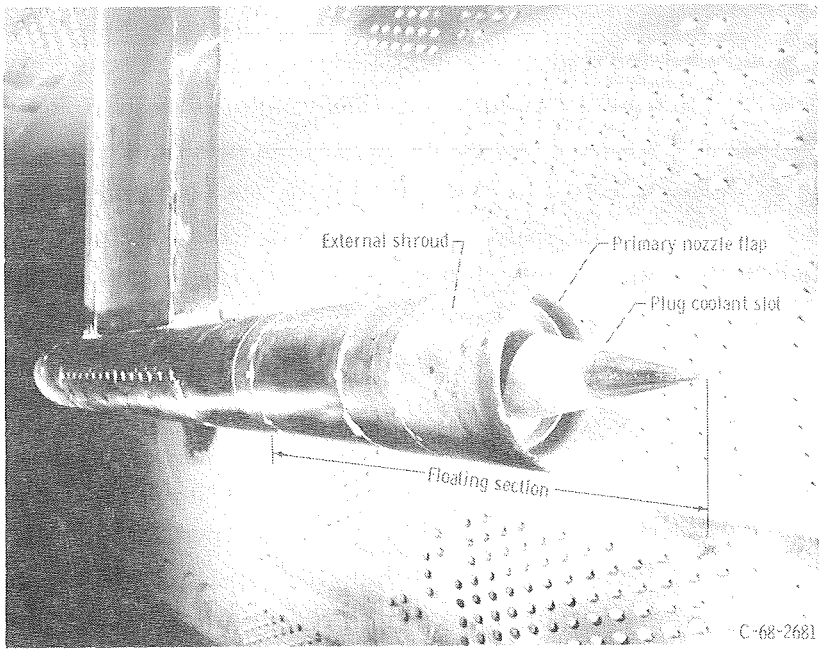

Figure 1. - Installation of model in 8- by 6-Foot Supersonic Wind Tunnel.

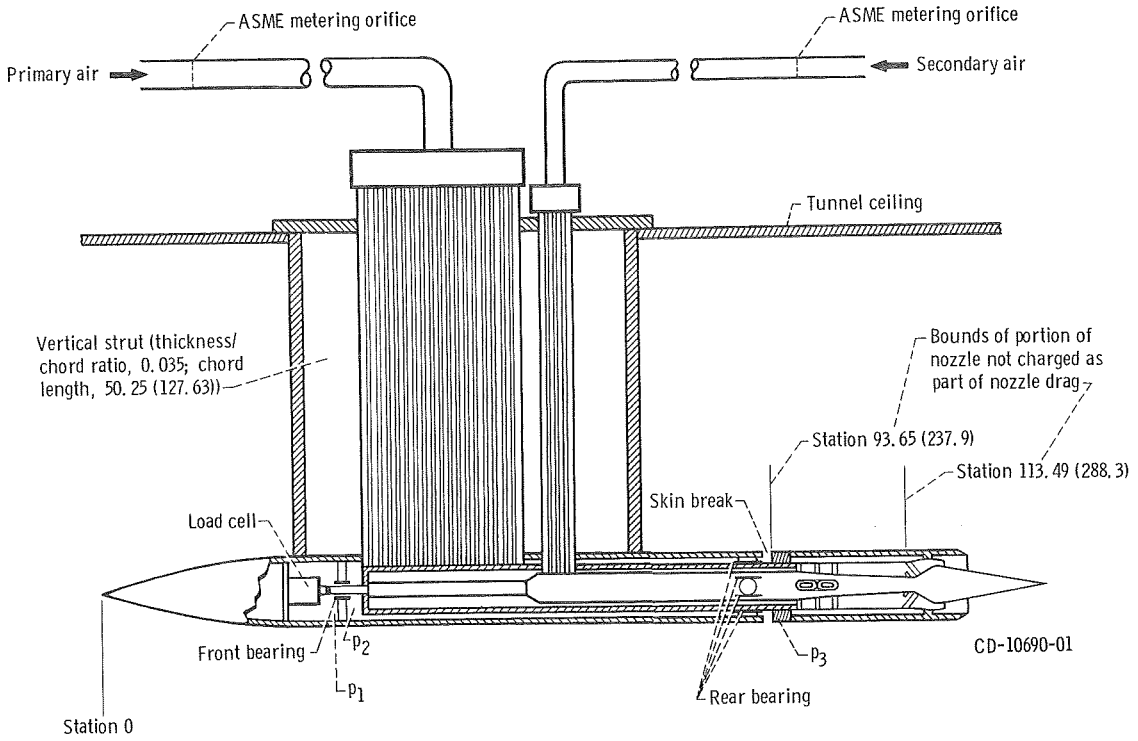

Figure 2. - Schematic view of 8.5-inch (21.6-cm) jet exit model and air supply systems for 8- by 6-foot supersonic wind tunnel. (All dimensions are in inches (cm).)

manifolds located outside of the test section. The air bottles were supported by front and rear bearings. The axial forces acting on the floating portions of the model were transmitted to the load cell located in the nose of the model. A water cooled jacket surrounded the load cell and maintained a constant temperature of 90° F (305.5 K) to eliminate errors in the calibration caused by variations in model temperature from aerodynamic heating. A static calibration of the load cell was obtained by applying known forces to the floating section and measuring the output of the load cell.

The load cell readings were corrected for internal tare forces using the measured tare pressures (p_1, p_2, and p_3) shown in figure 2. The load cell measured the axial force acting on the floating section of the model. This force included internal thrust and the external drag acting downstream of station 93.65, the location of the skin break. The model was tested only at zero angle of attack.

The nozzle performance excludes the friction drag on the cylindrical portion of the floating section between stations 93.65 and 113.49. The downstream end of this section was arbitrarily selected as being 0.75 model diameter upstream of the nozzle throat and was, therefore, considered to be the nozzle attachment station. The friction drag on the model between stations 93.65 and 113.49 was calculated using the semiempirical, flat-plate, local skin-friction coefficient from reference 3. The coefficient accounts for variations in boundary layer thickness and flow profile with Reynolds number and free stream Mach number. Previous measurements of the boundary layer characteristics at the aft end of this jet exit model (ref. 4) indicated that the profile and thickness were essentially the same as that computed for a flat plate of equal length. The ratio of measured boundary layer momentum thickness to model diameter was about 0.020 for the jet exit model over the range of Mach numbers. The strut wake appeared to affect only a localized region near the top of the model and resulted in a lower local free stream velocity than measured on the side and the bottom. Therefore, the results of reference 3 were used without corrections for three-dimensional flow or strut interference effects. The calculated friction drag was, therefore, added to the load cell reading to obtain the overall thrust minus drag of the exhause nozzle.

Primary and coolant air were provided by means of air-flow supply lines which entered the model through the hollow support strut (fig. 2). Both flow rates were measured by means of standard ASME sharp edge flow metering orifices located in the external supply lines. These flows were brought through the strut at high pressure and velocity to minimize tube diameters and thus to maintain a thin strut. Both flows entered the model at right angles to the force axis, which eliminated the need to account for any inlet momentum forces. A uniform primary flow was maintained by using choke

plates and screens upstream of the nozzle inlet station. An ideal primary flow was also calculated as that passing through the choked geometric area at the measured total pressure and temperature. The ideal flow was compared to the measured primary flow to determine a discharge coefficient for this primary configuration. The results indicated that the discharge coefficient was constant, over the range of pressure ratios tested, at a value of $C_{d,8} = 0.975$, except with the coolant slot located upstream of the primary throat. Even with no coolant injection the primary pressure distribution was different for the upstream slot location and yielded a lower discharge coefficient. Both the coolant flow rate and the ratio of coolant exit area to primary throat area affected the coefficient (fig. 3). Coolant injection reduced $C_{d,8}$ below the value it had with no injection. This

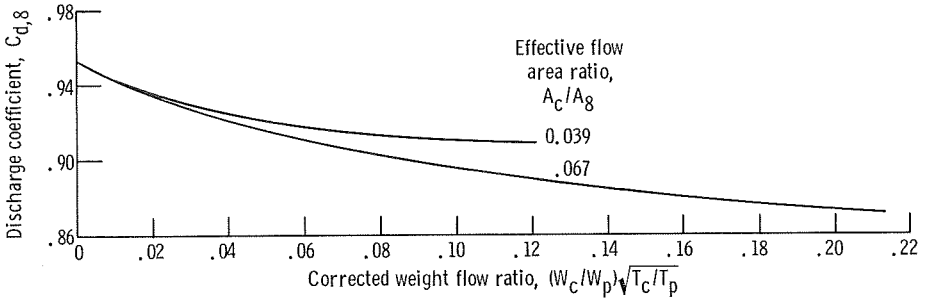

Figure 3. - Effect of coolant weight flow on primary flow coefficient for coolant slots located at $x/l = -0.10$.

injection effect was greater for the larger coolant exit area than for the smaller exit area. The secondary air in the central air bottles was ducted to the nozzle plug and was used to simulate the coolant flow. No secondary air was provided in the annulus between the primary flap and external cylindrical shroud, as is usually done with a nozzle of this type (ref. 1). Both the primary and coolant flows were maintained at room temperature.

Since the ambient pressure is constant in the wind tunnel for a given free stream Mach number, nozzle pressure is varied by changing the internal total pressure up to a maximum based on model strength. Maximum nozzle pressure ratios varied from 4.0 at Mach 0 to about 20 at Mach 1.97. Coolant flows were varied during the test up to a maximum value of 20 percent of the primary flow rate.

The ideal thrust for both the primary and coolant flow was calculated from the measured mass flow rates expanded from their measured total pressures to p_0. Nozzle efficiency is defined as the ratio of the measured thrust minus drag to the ideal thrust of both the primary and coolant flows:

$$\text{nozzle efficiency} = \frac{F - D}{F_{i,p} + F_{i,c}}$$

Nozzle Configuration

The basic configuration used in the coolant study was a 10° half-angle conical plug nozzle (ref. 1). This nozzle consisted of a rigid plug with variations in nozzle throat area for an afterburning turbojet engine provided by an iris-type primary flap. This nozzle was designed for a supersonic cruise aircraft and had an overall design pressure ratio of 26.3 with the afterburner off. The primary throat was only tested in the maximum afterburning position in the current test. This fixed area was 40 percent larger than the afterburner off area and had a ratio of throat to maximum model area of 0.36. Basic model dimensions are shown in figure 4. In the afterburning position the conical

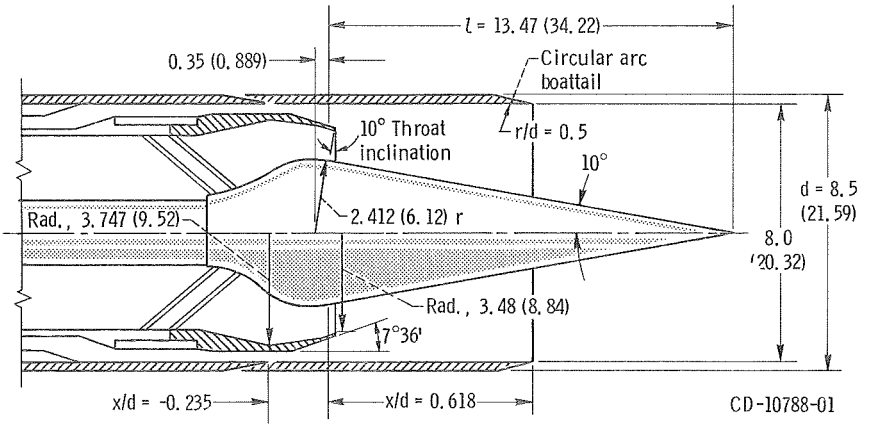

Figure 4. - Plug nozzle configuration details.

primary flap had a boattail angle of $7^{\circ}36'$ and a ratio of flap area to model area of 0.13. A secondary flow area was provided between the primary and outer shrouds. The minimum secondary flow area was constant and equal to about 8.3 percent of the model area. No secondary flow was provided in this test. The results presented in reference 1 have shown that secondary flow in this nozzle type can significantly improve nozzle performance at all Mach numbers. However, since this jet exit model only provided two flows, the secondary flow was used to simulate coolant flow to the central plug.

A simulated translating outer cylindrical shroud was used to vary the internal expansion ratio of this plug nozzle. The shroud is retracted at takeoff and at subsonic speeds but is extended for higher speeds and pressure ratios. The results of reference 1 have indicated that a two position shroud can provide near optimum nozzle efficiency over a Mach number range from 0 to 2.0. Therefore, in the current test program the external shroud was only tested in two positions. The shroud was retracted at Mach num-

bers from 0 to 1.2 and extended at Mach numbers from 1.2 to 1.97. The two shroud locations tested are shown in figure 4. The shroud location is referenced to the nozzle throat station. The internal area and pressure ratios for the two locations tested are shown in table I for this afterburning configuration. The outer shrouds were provided with circular arc boattails to minimize drag and had a ratio of boattail to model area of 0.115.

TABLE I. - SHROUD VARIABLES

[Overall design: pressure ratio, 26.3; area ratio, 3.43.]

Ratio of shroud axial length to diameter, x/d_{max}	Internal expansion pressure ratio, P_7/P_9	Internal area ratio, A_9/A_8
-0.235	1.89	1.00
.618	11.93	2.13

Coolant Configurations

Details of the coolant configurations tested are shown in figure 4. Coolant slots were tested at three locations on the plug surface, two downstream of the throat (figs. 5(a) and (b)), and one upstream of the throat (fig. 5(c)). Effective flow area ratios (Ac/Ap) for these slots were calculated from the data when the slots were choked. The film coolant slot located at the 50 percent point on the plug (fig. 5(a)), had an effective flow area equal to 2.8 percent of the primary flow area. For this slot location an alternate configuration was also used to simulate a convectively cooled plug truncated to half-length with the coolant flow dumped into the plug base. The conical tip insert was removed, and a flat base insert was added (fig. 5(a)). The effective flow area of this configuration was 3.4 percent of the primary flow area. The effective flow area of the film coolant slot located at a point 10 percent downstream of the throat (fig. 5(b)) was 3.4 percent of the primary flow area. Two film coolant slots were tested upstream of the nozzle throat. Both slots were located at the same station (fig. 5(c)) and had effective flow areas equal to 3.9 and 6.7 percent of the primary flow area. Coolant total pressures were measured inside the plug at the locations shown in figure 5. Internal flow passages were such that the minimum flow area downstream of the secondary total pressure measuring station occurred at the coolant discharge point, which allowed the assumption of negligible secondary total pressure loss within the flow passages. Photographs of the various coolant configurations tested are shown in figure 6. A summary of the cooling configuration variables tested is presented in table II.

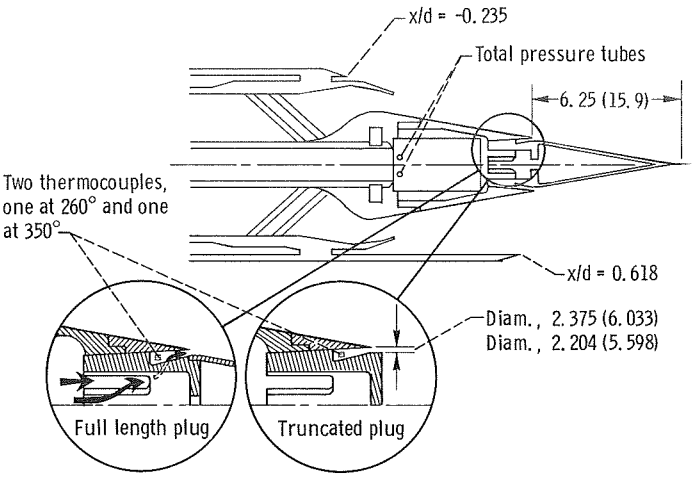

(a) Full length and truncated plugs; coolant slot location x/ℓ, 0.50.

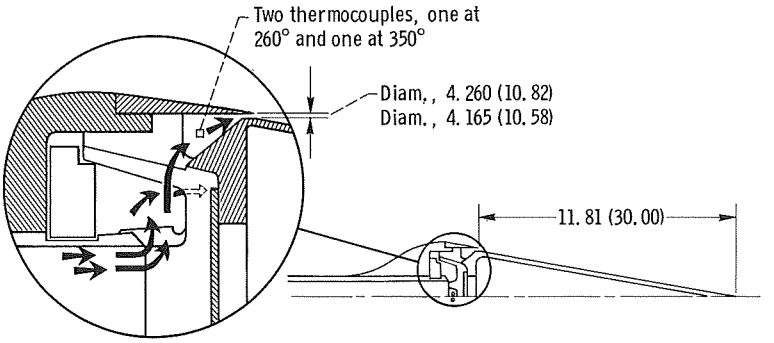

(b) Full length plug; coolant slot location x/ℓ, 0.10.

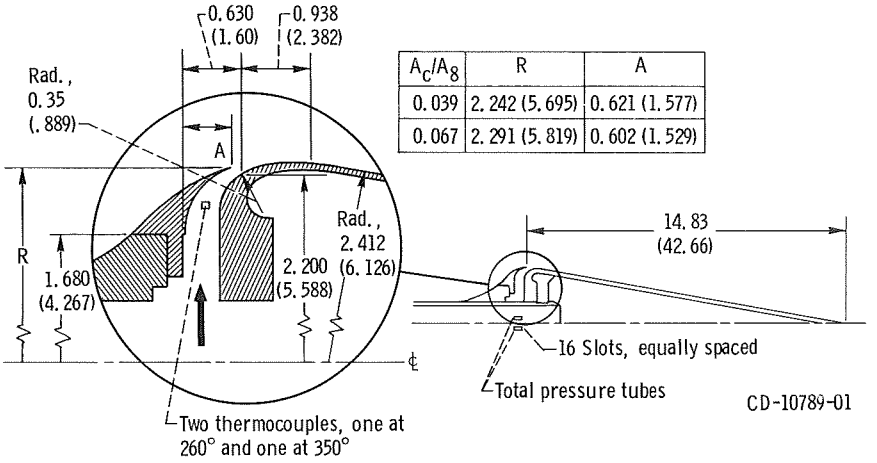

A_c/A_8	R	A
0.039	2.242 (5.695)	0.621 (1.577)
0.067	2.291 (5.819)	0.602 (1.529)

(c) Full length plug; coolant slot location, x/ℓ, -0.10.

Figure 5. - Coolant slot configuration details. (All dimensions are in inches (cm).)

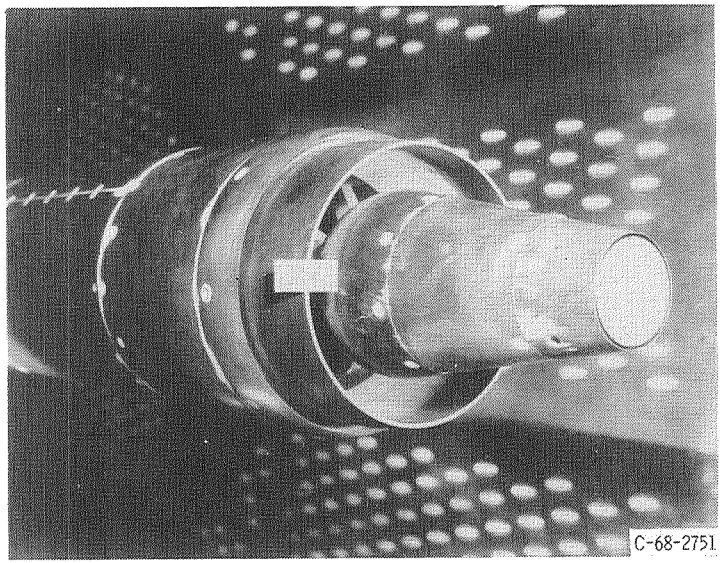

(a) Slot location x/l, 0.50; truncated plug; effective flow area ratio A_c/A_8, 0.034.

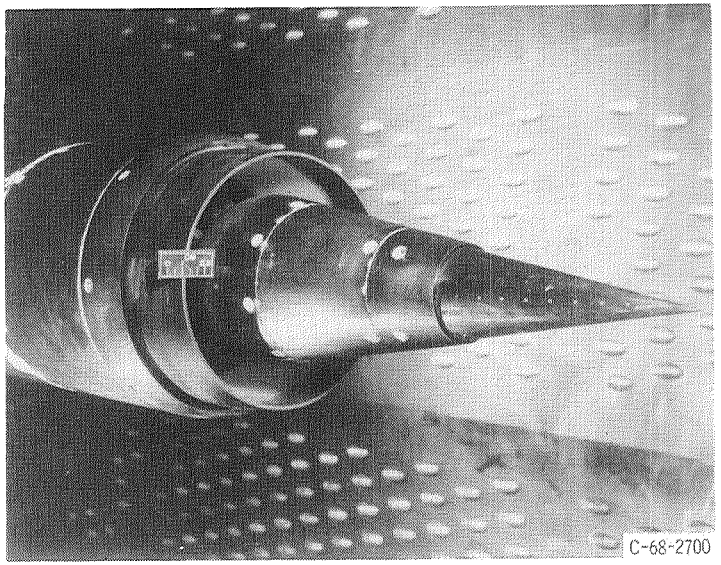

(b) Slot location x/l, 0.50; full length plug; effective flow area ratio A_c/A_8, 0.028.

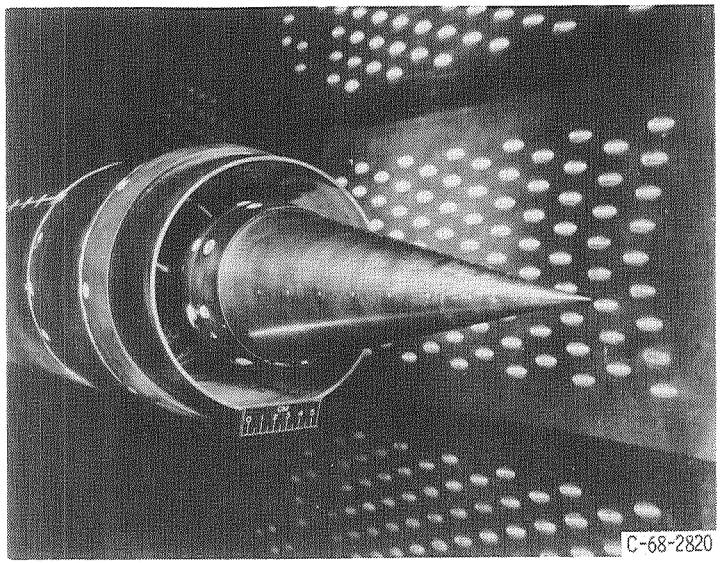

(c) Slot location x/l, 0.10; full length plug; effective flow area ratio A_c/A_8, 0.034.

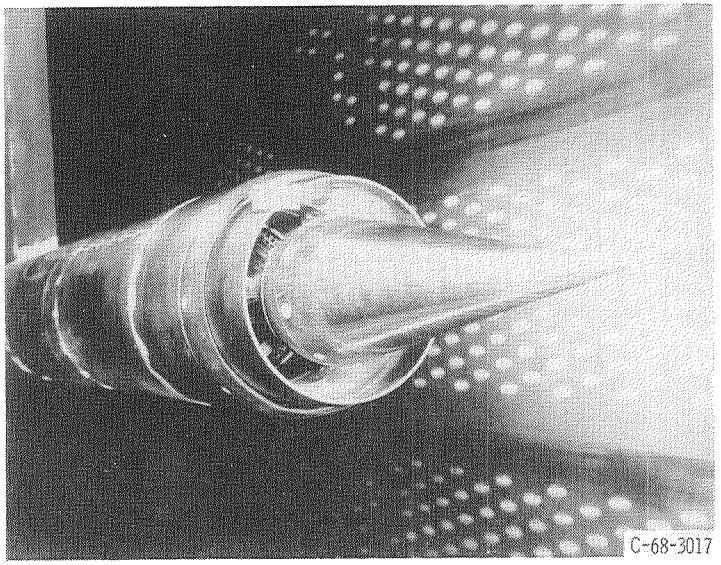

(d) Slot location x/l, 0.10; full length plug; effective flow area ratio A_c/A_8, 0.039 or 0.067.

Figure 6. - Plug cooling configurations.

TABLE II. - COOLING CONFIGURATION VARIABLES

Type of cooling	Coolant slot location, x/l	Effective coolant flow area ratio, A_c/A_8
Convective	0.50	0.034
Film	.50	.028
Film	.10	.034
Film	-.10	.039
Film	-.10	.067

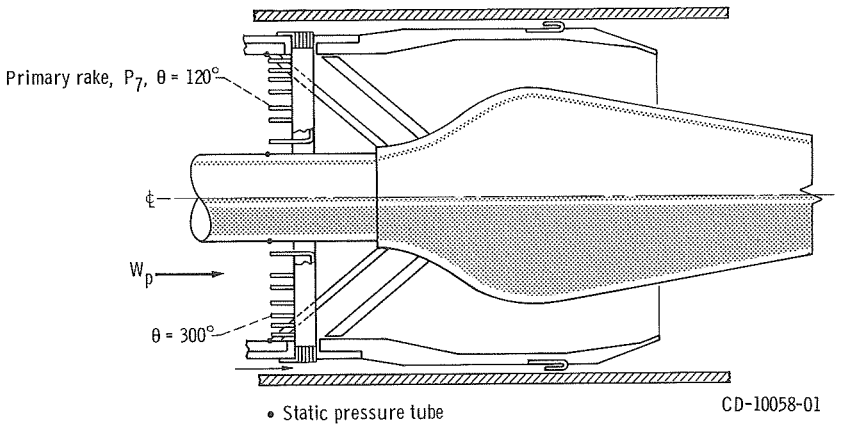

(a) Primary rake.

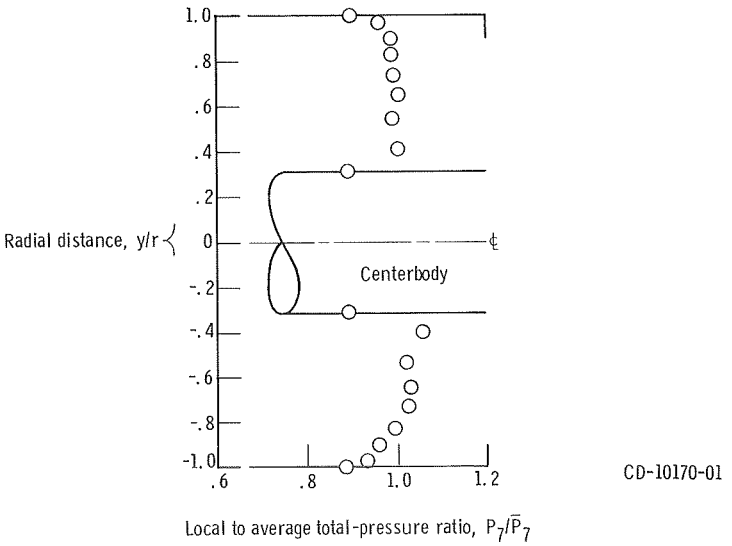

(b) Typical primary rake pressure profile (ref. 1).

Figure 7. - Primary flow instrumentation and pressure profile.

Instrumentation

The primary total pressure was obtained by the use of the total pressure rake shown in figure 7(a). The two primary rakes were area weighted to facilitate the calculation of the average total pressure. With the afterburner on, the calculated one-dimensional Mach number at the rake station was 0.46. A typical primary pressure profile is shown in figure 7(b).

RESULTS AND DISCUSSION

The basic data, consisting of nozzle efficiencies and pumping characteristics, are presented in appendix B for the five coolant configurations tested. These basic data plots were then used in conjunction with an assumed typical pressure ratio schedule (fig. 8) to

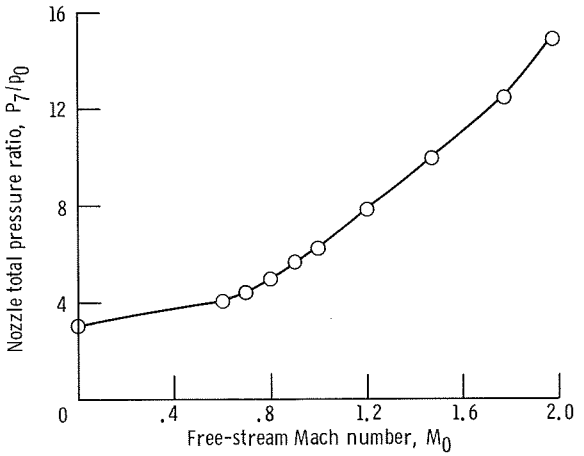

Figure 8. - Assumed nozzle pressure ratio schedule for typical afterburning turbojet engine.

present the nozzle performance and comparisons in the remaining figures. These presentations are further limited to an assumed coolant corrected flow of 2 percent. Performance characteristics at other coolant flow rates can be obtained from the basic data shown in appendix B.

Effect of Coolant Location on Nozzle Performance

The effect of coolant slot location is shown in figure 9 at takeoff and at three typical acceleration conditions, Mach numbers 0.9, 1.2, and 1.97. Nozzle efficiency and pump-

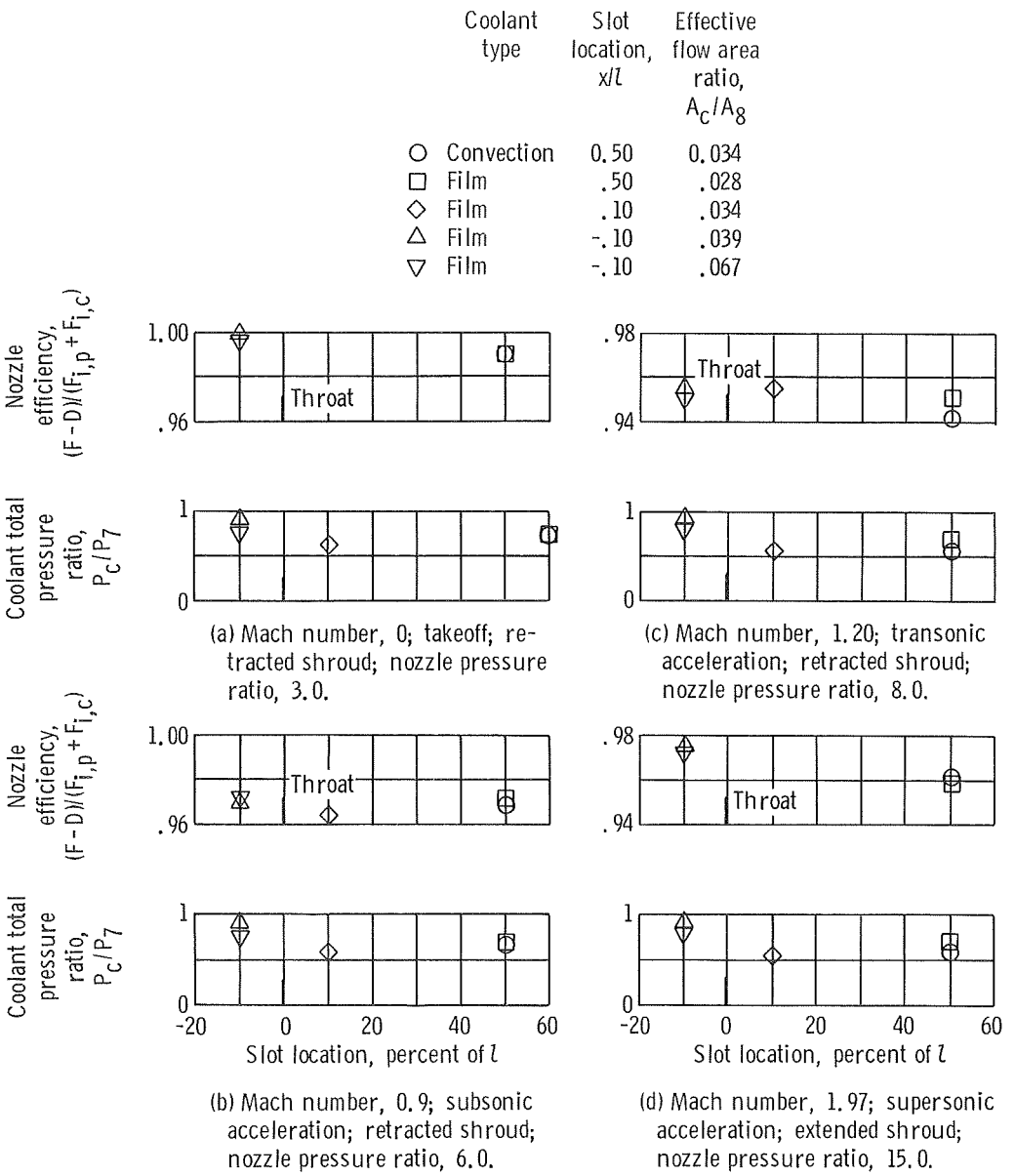

(a) Mach number, 0; takeoff; retracted shroud; nozzle pressure ratio, 3.0.

(c) Mach number, 1.20; transonic acceleration; retracted shroud; nozzle pressure ratio, 8.0.

(b) Mach number, 0.9; subsonic acceleration; retracted shroud; nozzle pressure ratio, 6.0.

(d) Mach number, 1.97; supersonic acceleration; extended shroud; nozzle pressure ratio, 15.0.

Figure 9. - Effect of cooling slot location on nozzle efficiency and pumping characteristics for corrected weight flow ratio of 0.02.

ing requirements are shown for the specified nozzle pressure ratio and a corrected coolant flow ratio of 2 percent. The external cylindrical shroud was retracted at Mach numbers of 0, 0.9, and 1.2 and extended at Mach 1.97.

At takeoff and at the three typical acceleration conditions, all coolant configurations had nozzle efficiencies within 1.5 percent of each other. The coolant slots located upstream of the nozzle throat generally provided the highest nozzle efficiency but also required the highest coolant pressures. Nozzle efficiencies were generally high at these four flight conditions. For example, nozzle efficiencies were generally 99 percent or better at takeoff, between 94 and 95.5 percent at transonic acceleration, and between 96 and 97.5 percent at Mach 1.97. It is suggested that secondary flow between the primary and outer shrouds would have improved the nozzle efficiency, based on results presented in reference 1. The convection cooled truncated plug generally had performance equal to or slightly lower than a film cooled configuration at the same location.

In figure 9 the coolant total pressure ratios at subsonic Mach numbers were very nearly equal for the convection and film cooling slots at the 50 percent location, though the effective flow areas differed by about 20 percent. Examination of the data plots in appendix B (figs. 11 and 12) indicates that the coolant slot was not choked for the truncated plug at subsonic conditions. Otherwise all coolant slots downstream of the throat were generally choked with a corrected weight flow ratio of 2 percent.

Coolant total pressures required at these locations were generally equal to 70 to 75 percent of the primary total pressure. A similar sized slot upstream of the throat was not choked and required a total pressure about equal to the primary total pressure. This coolant pressure was reduced to about 80 percent of the primary total pressure by increasing the effective coolant flow area by 70 percent. This increase in slot area resulted in a slight loss in nozzle efficiency, generally less than 1/2 percent.

Effect of Mach Number on Performance

The nozzle efficiency and pumping characteristics are shown in figure 10 (at Mach numbers from 0 to 1.97) for each of the five coolant configurations. This performance also is for the assumed pressure ratio schedule shown in figure 8 and for a corrected coolant weight flow ratio of 2 percent. The external cylindrical shroud was retracted for Mach numbers from 0 to 1.2 and extended for Mach numbers from 1.2 to 1.97.

For the typical turbojet acceleration schedule, all cooling configurations provided high nozzle efficiency at Mach numbers from 0 to 1.97. For example, nozzle efficiency typically varied from 99 percent at takeoff to a minimum of about 95 percent at Mach 1.2 and then increased to about 97 percent at Mach 1.97. The efficiencies at takeoff and Mach 1.77 were obtained at pressure ratios near the internal expansion pressure ratio

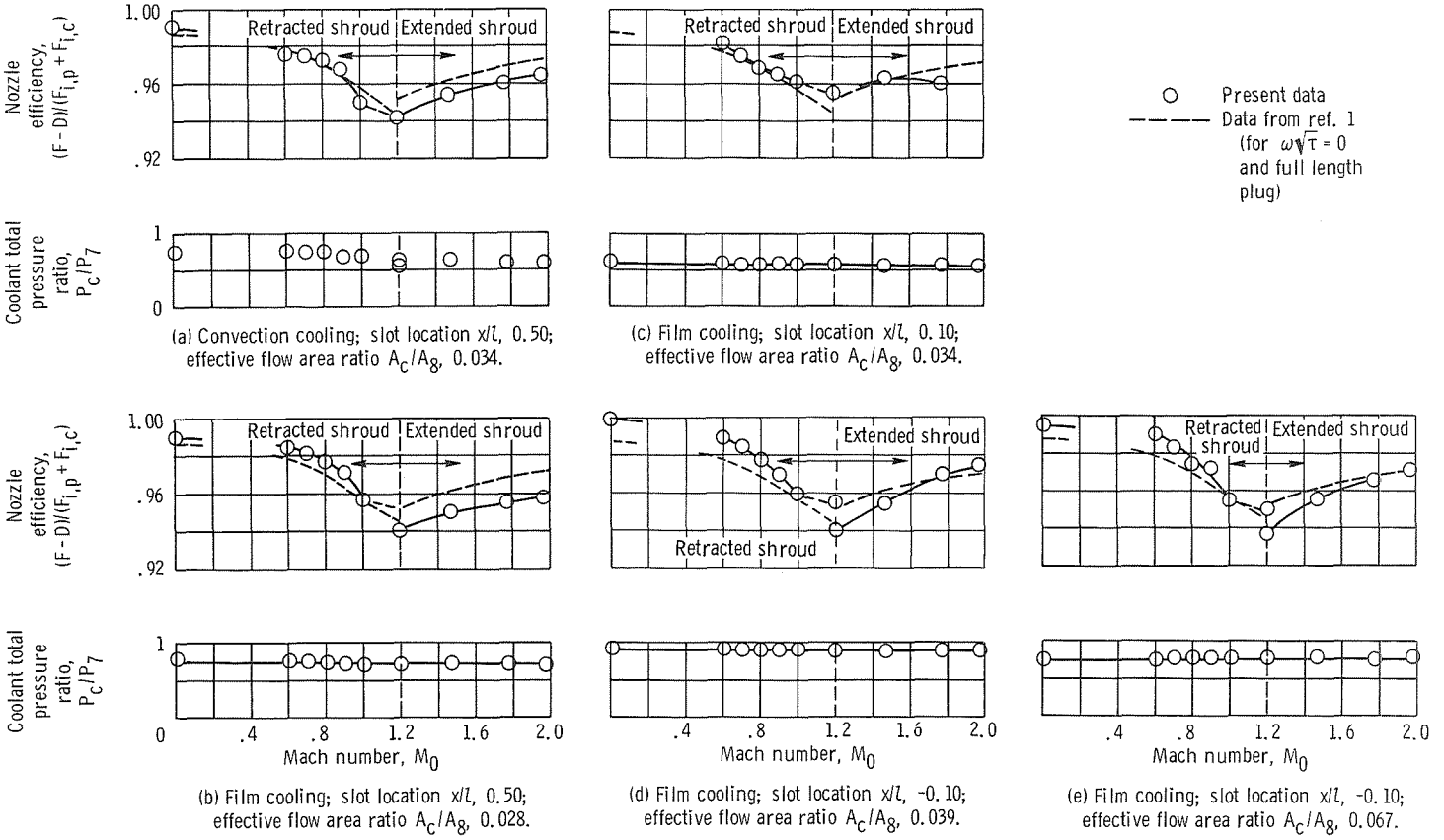

(a) Convection cooling; slot location x/l, 0.50; effective flow area ratio A_c/A_8, 0.034.

(c) Film cooling; slot location x/l, 0.10; effective flow area ratio A_c/A_8, 0.034.

(b) Film cooling; slot location x/l, 0.50; effective flow area ratio A_c/A_8, 0.028.

(d) Film cooling; slot location x/l, -0.10; effective flow area ratio A_c/A_8, 0.039.

(e) Film cooling; slot location x/l, -0.10; effective flow area ratio A_c/A_8, 0.067.

Figure 10. - Performance and pumping characteristics of cooling configurations over assumed flight trajectory for corrected weight flow ratio of 0.02.

values with the external shroud retracted and extended, respectively.

Peak nozzle efficiency at Mach 1.2 was obtained with the shroud retracted rather than extended. An intermediate shroud location may have provided higher efficiency at this Mach number based on results presented in reference 1.

Data from reference 1 are included in figure 9 for comparison. The wind tunnel model used in reference 1 was modified for the present plug cooling investigations. With zero secondary flow it corresponds closely to the configurations in the present test. The shroud positions for the results of reference 1 which are plotted here were identical to the shroud positions in the present test. A configuration with afterburner on and 50 percent truncated plug was not tested in reference 1, however, so the full length plug data are plotted for all configurations in figure 10.

The present data generally agreed with the data of reference 1 within 1.5 percent for all configurations. At subsonic conditions they tend to be higher than the reference 1 data, and at supersonic conditions they tend to be lower.

Coolant total pressure requirements were generally insensitive to free stream Mach number variations for any specified coolant location. As discussed in the preceding paragraphs, coolant pressure requirements increased when the slots were moved upstream of the nozzle throat. Also, the configurations with slots upstream of the throat station generally provided the optimum nozzle efficiency over the range of Mach numbers tested (figs. 10(d) and (e)).

SUMMARY OF RESULTS

An experimental investigation was conducted to determine the coolant flow effects on the performance of a low angle conical plug nozzle designed for a supersonic cruise aircraft. The primary throat area was fixed in the maximum afterburning position with a throat to nacelle area ratio of 0.36. Film coolant slots were evaluated at three locations on the plug surface, one upstream of the nozzle throat and two downstream. An alternate configuration simulated a convectively cooled plug truncated to half-length with the coolant flow dumped into the plug base. The following results were obtained over a range of Mach number from 0 to 1.97 at a constant corrected coolant flow rate of 2 percent of the primary flow and no secondary flow between the primary nozzle and the cylindrical shroud:

1. At takeoff and at three typical acceleration conditions (Mach 0.9, 1.2, and 1.97) all configurations had nozzle efficiencies within 1.5 percent of each other. The coolant slot upstream of the nozzle throat generally provided the highest nozzle efficiency but also required the highest coolant pressures.

2. For a typical turbojet acceleration schedule all cooling configurations provided high nozzle efficiency at Mach numbers from 0 to 1.97. For example, nozzle efficiency typically varied from 99 percent at takeoff to a minimum of about 95 percent at Mach 1.2 and then increased to about 97 percent at Mach 1.97.

3. All coolant slots downstream of the throat were generally choked and required coolant total pressures of about 75 percent of the primary total pressure. A similar sized slot upstream of the throat was not choked for 2 percent cooling flow and required a total pressure about equal to the primary total pressure. This coolant pressure was reduced to about 80 percent of the primary total pressure by increasing the effective coolant flow area by 70 percent. This increase in slot area resulted in a slight loss in nozzle efficiency.

Lewis Research Center,
National Aeronautics and Space Administration,
Cleveland, Ohio, May 7, 1970,
720-03.

APPENDIX A

SYMBOLS

A	area
C_d	discharge coefficient
D	drag
d	model diameter
F	thrust
l	full plug length measured from nozzle throat
M	Mach number
P	total pressure
p	static pressure
r	radius
T	total temperature
W	weight flow rate
x	axial distance measured from nozzle throat
θ	circumferential position
$\frac{W_c}{W_p}\sqrt{\frac{T_c}{T_p}}$	corrected secondary flow rate ratio

Subscripts:

c	coolant
i	ideal
max	maximum
p	primary
x	condition of distance x
0	free stream
1	internal tare station (see fig. 2)
2	internal tare station (see fig. 2)
3	internal tare station (see fig. 2)
7	nozzle inlet
8	nozzle throat
9	nozzle exit

APPENDIX B

NOZZLE EFFICIENCY AND PUMPING CHARACTERISTICS

This appendix contains all of the nozzle efficiency and pumping data for all five coolant configurations tested. For each configuration data are presented as a function of corrected coolant weight flow ratio, which ranged from zero to 20 percent of the primary flow. Results are shown for several Mach numbers between 0 and 1.2 with the external shroud retracted and from 1.2 to 1.97 with the shroud extended. At each Mach number tested the nozzle pressure ratio was varied about values corresponding to a typical schedule assumed for an afterburning turbojet engine (fig. 7). The following table summarizes the data presented in this section:

Figure	Coolant configuration	Slot location, x/l	Effective coolant flow area ratio, A_c/A_8
11	Convective	0.50	0.034
12	Film	.50	.028
13	Film	.10	.034
14	Film	-.10	.039
15	Film	-.10	.067

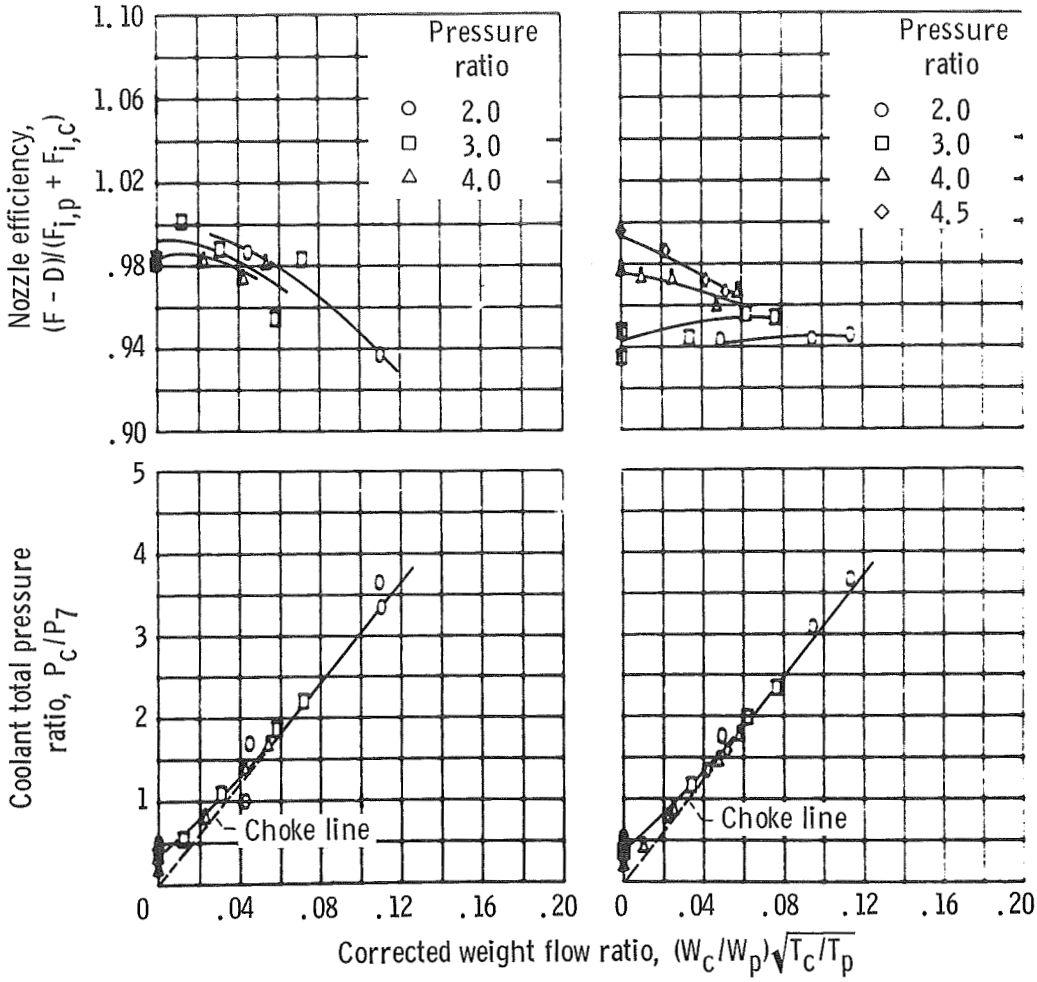

(a) Retracted shroud; Mach number, 0.

(b) Retracted shroud; Mach number, 0.6.

Figure 11. - Performance and pumping data. Truncated plug; slot location x/l, 0.50; effective flow area ratio A_c/A_8, 0.034.

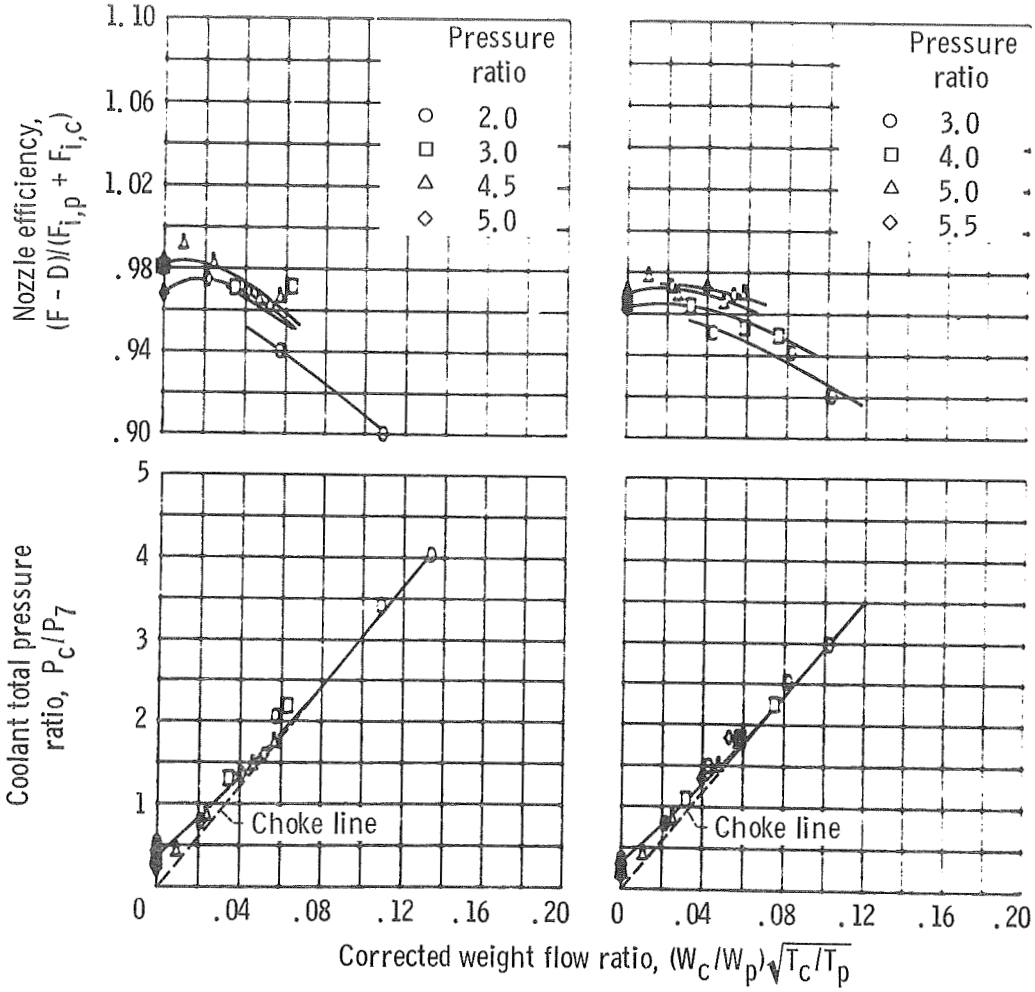

(c) Retracted shroud; Mach number, 0.7.

(d) Retracted shroud; Mach number, 0.8.

Figure 11. - Continued.

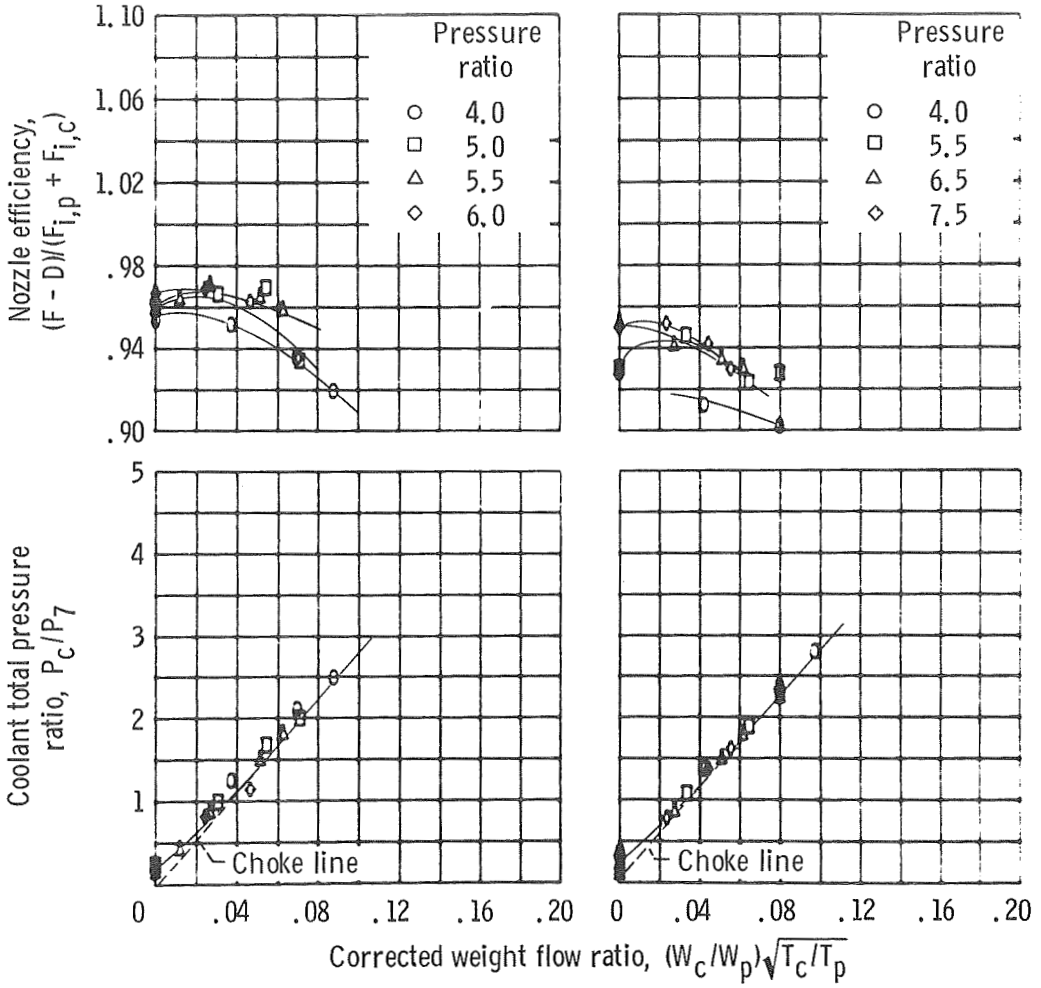

(e) Retracted shroud; Mach number, 0.9.

(f) Retracted shroud; Mach number, 1.0.

Figure 11. - Continued.

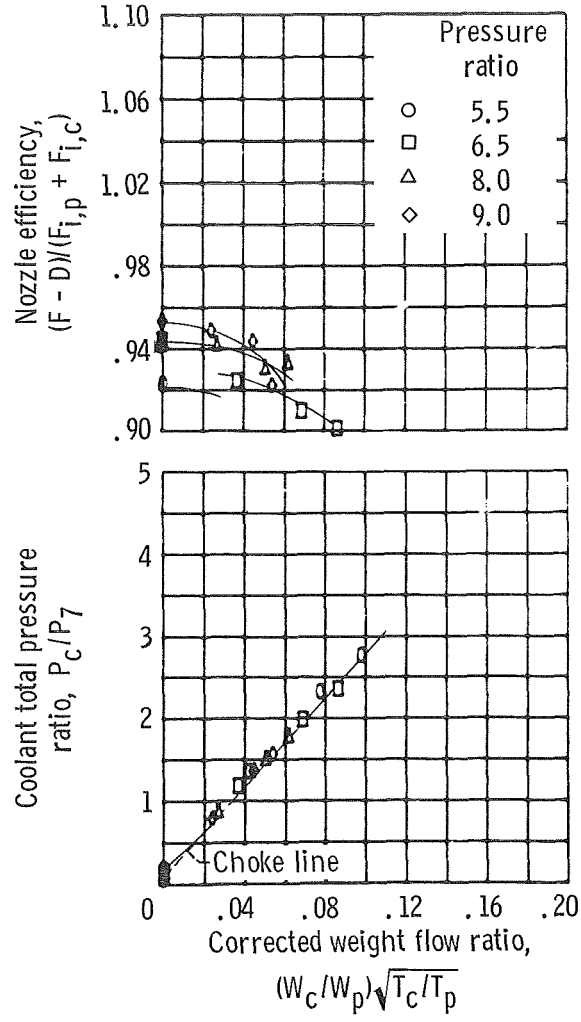

(g) Retracted shroud; Mach number, 1.2.

Figure 11. - Continued.

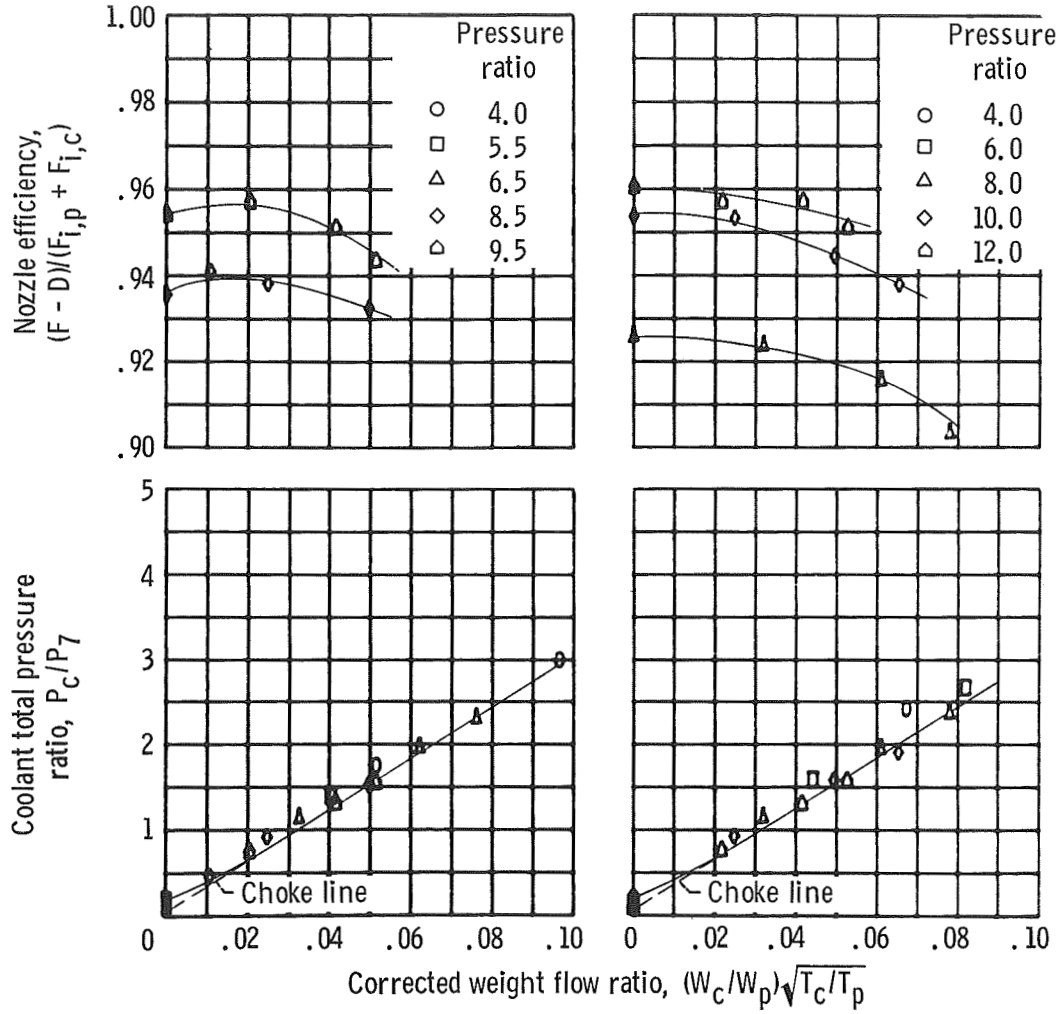

(h) Extended shroud; Mach number, 1.2.

(i) Extended shroud; Mach number, 1.47.

Figure 11. - Continued.

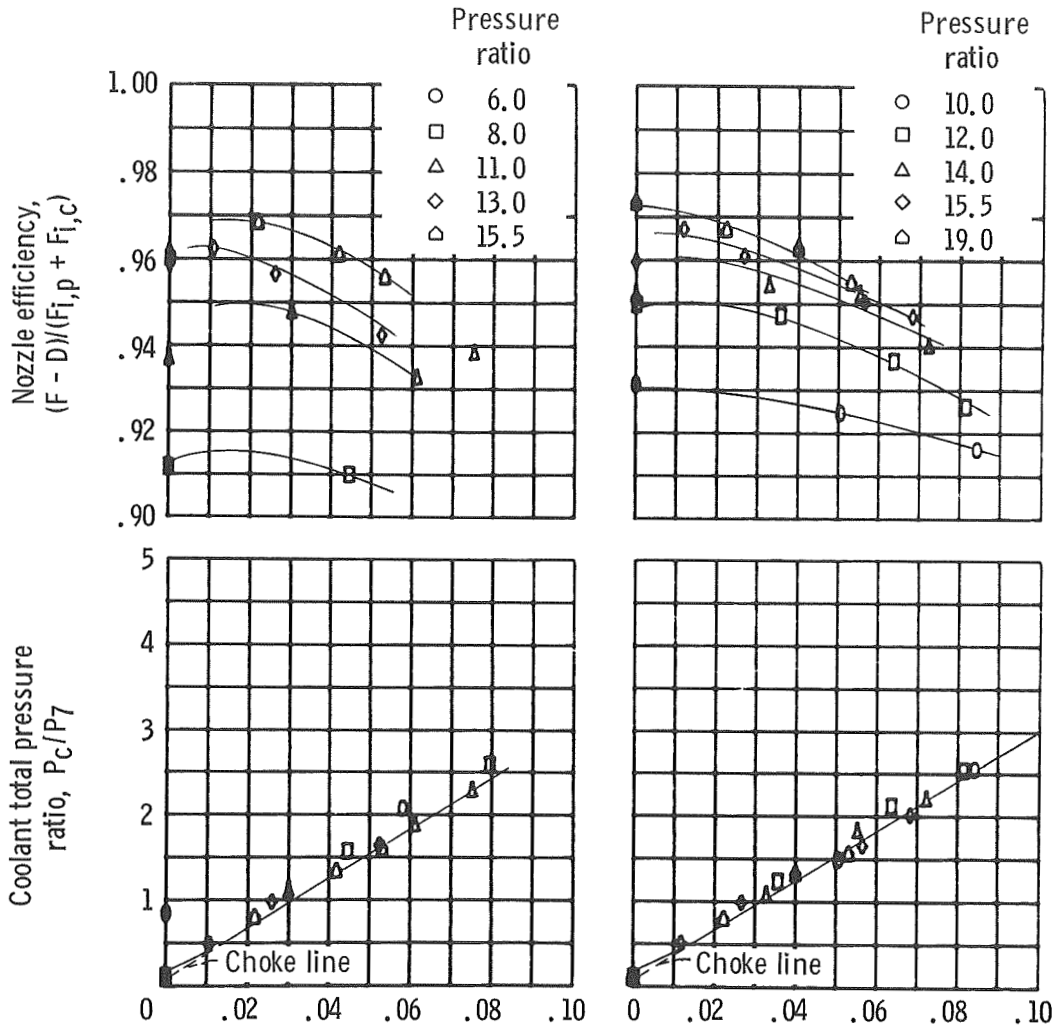

(j) Extended shroud; Mach number, 1.77.

(k) Extended shroud; Mach number, 1.97.

Figure 11. - Concluded.

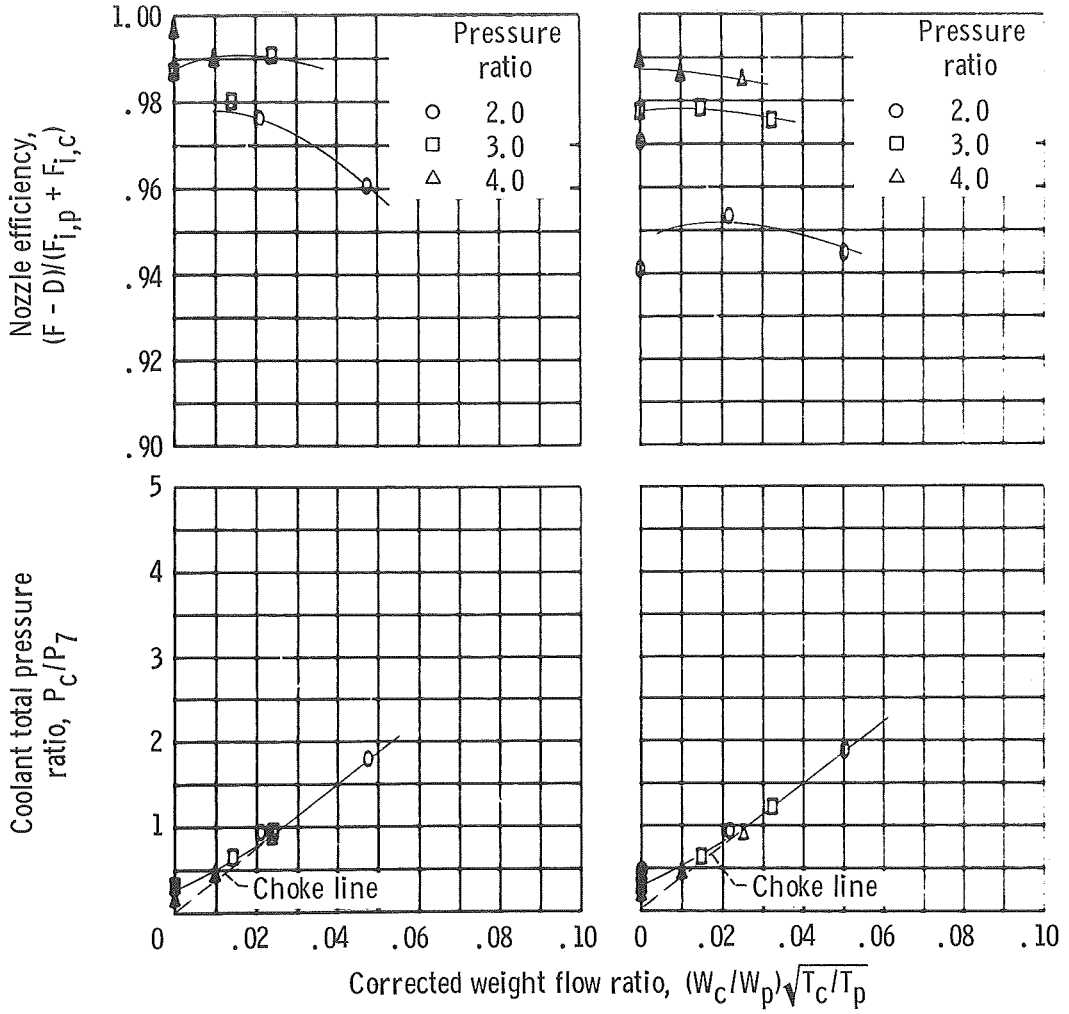

(a) Retracted shroud; Mach number, 0.

(b) Retracted shroud; Mach number, 0.6.

Figure 12. - Performance and pumping data. Full length plug; slot location x/l, 0.50; effective flow area ratio A_c/A_8, 0.028.

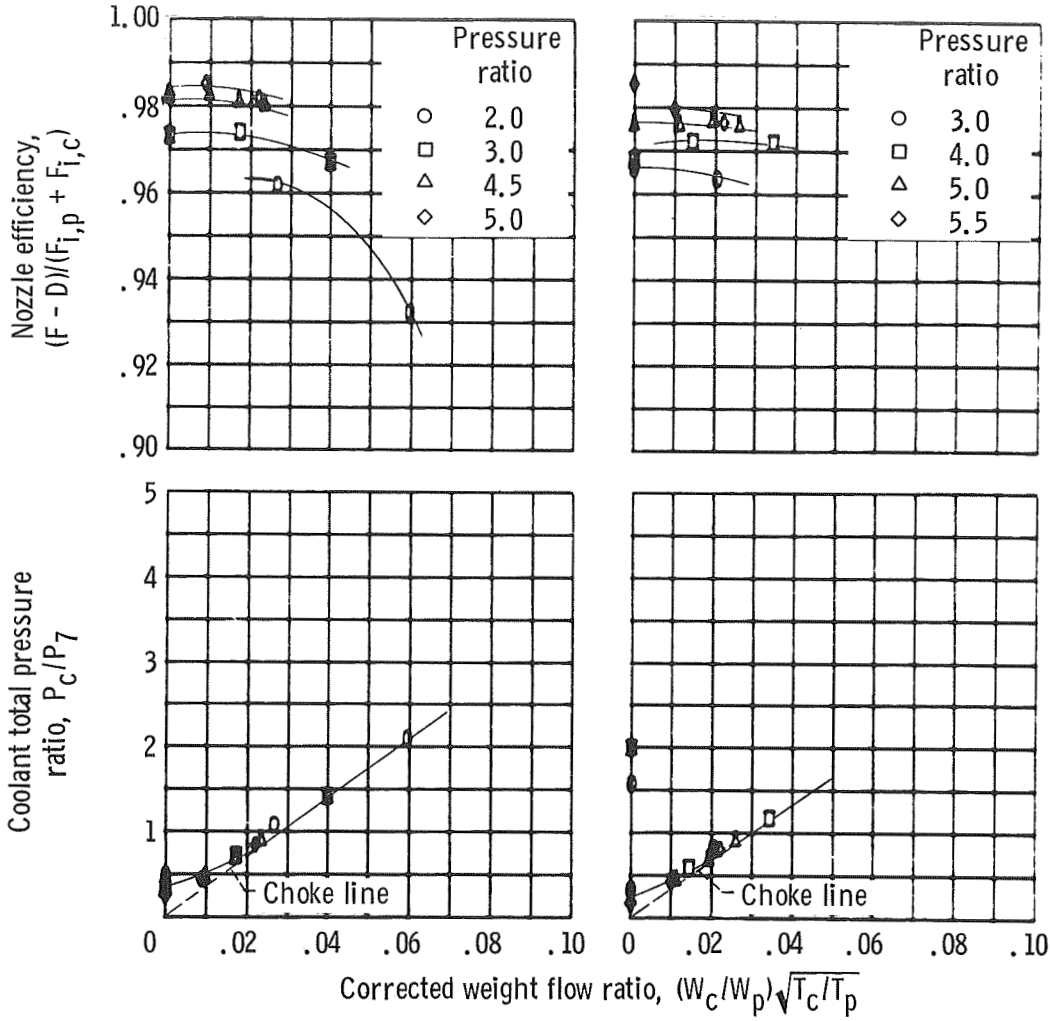

(c) Retracted shroud; Mach number, 0.7.

(d) Retracted shroud; Mach number, 0.8.

Figure 12. - Continued.

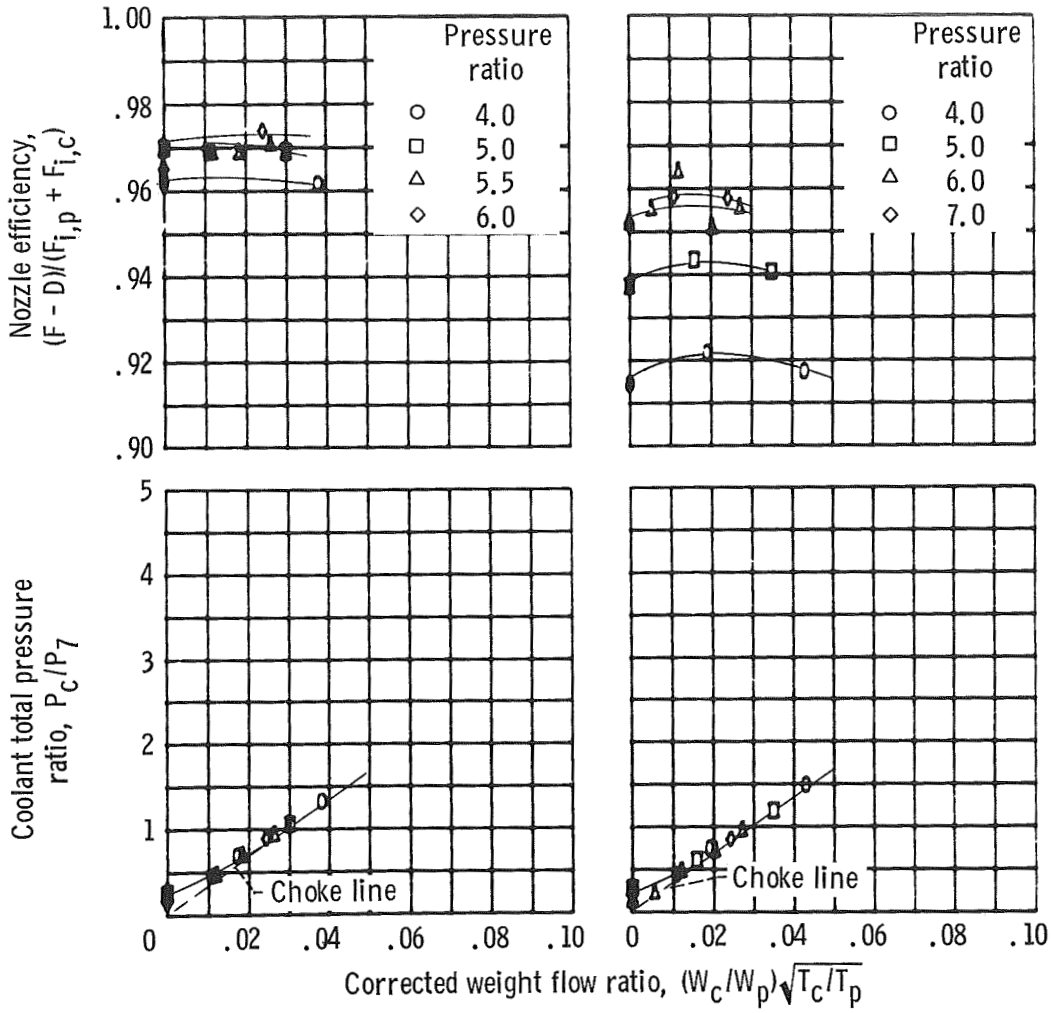

(e) Retracted shroud; Mach number, 0.9.

(f) Retracted shroud; Mach number, 1.0.

Figure 12. - Continued.

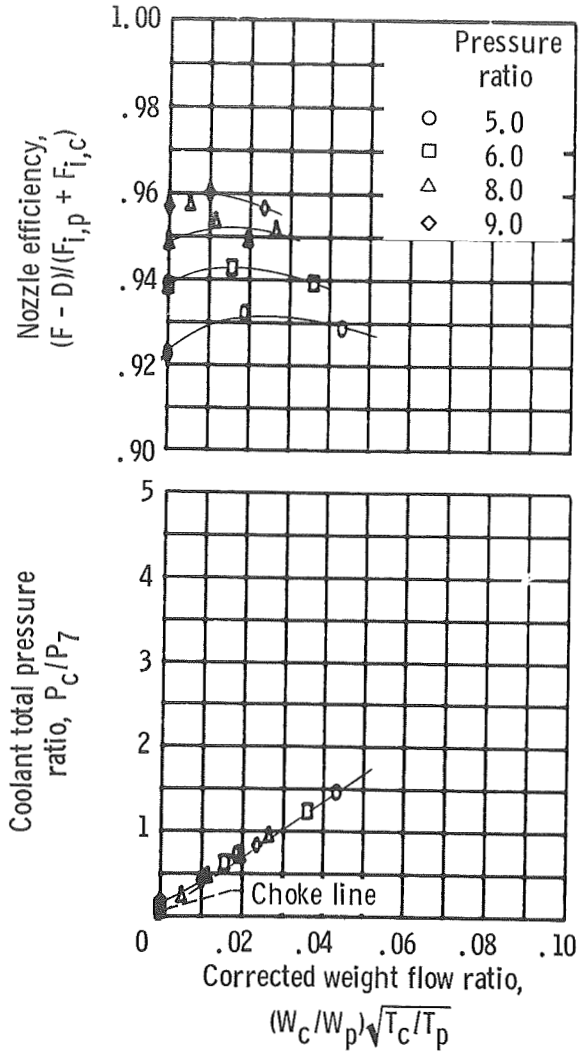

(g) Retracted shroud; Mach number, 1.2.

Figure 12. - Continued.

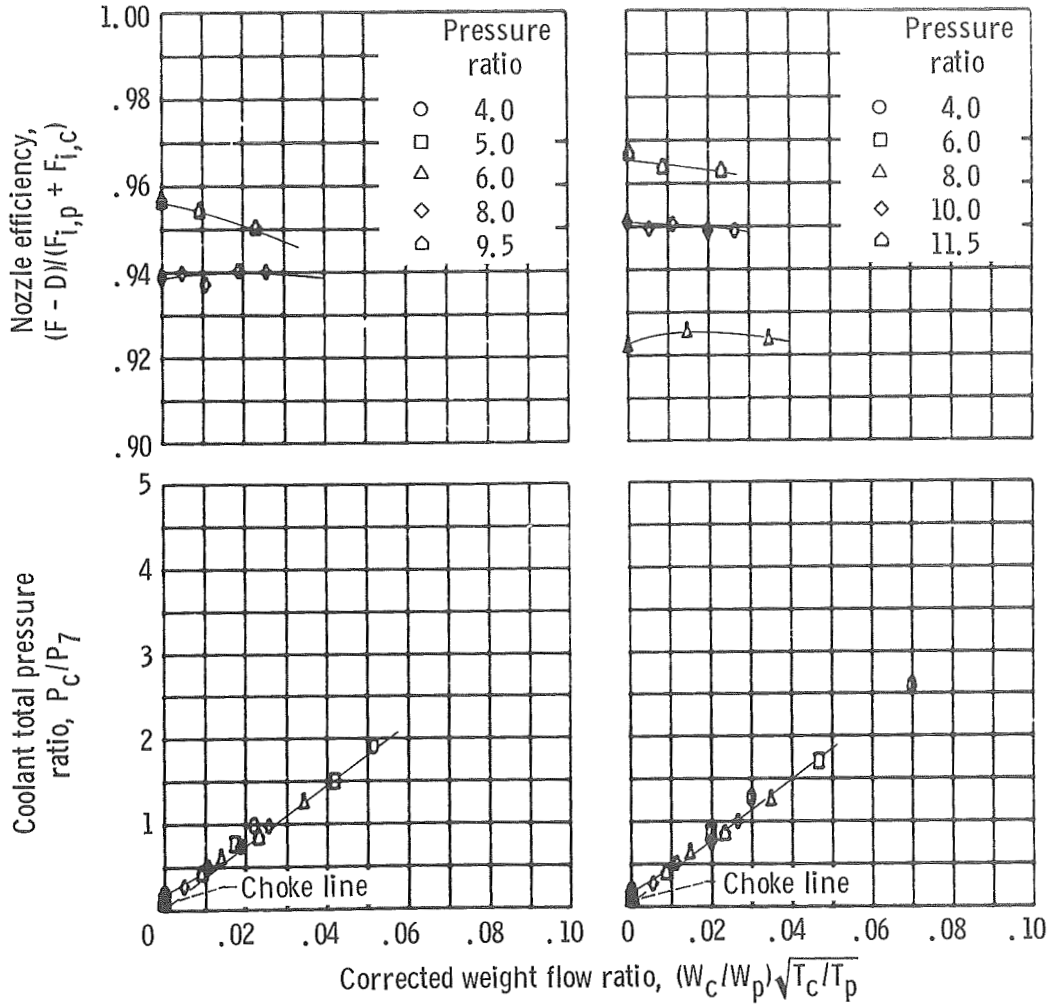

(h) Extended shroud; Mach number, 1.2.

(i) Extended shroud; Mach number, 1.47.

Figure 12. - Continued.

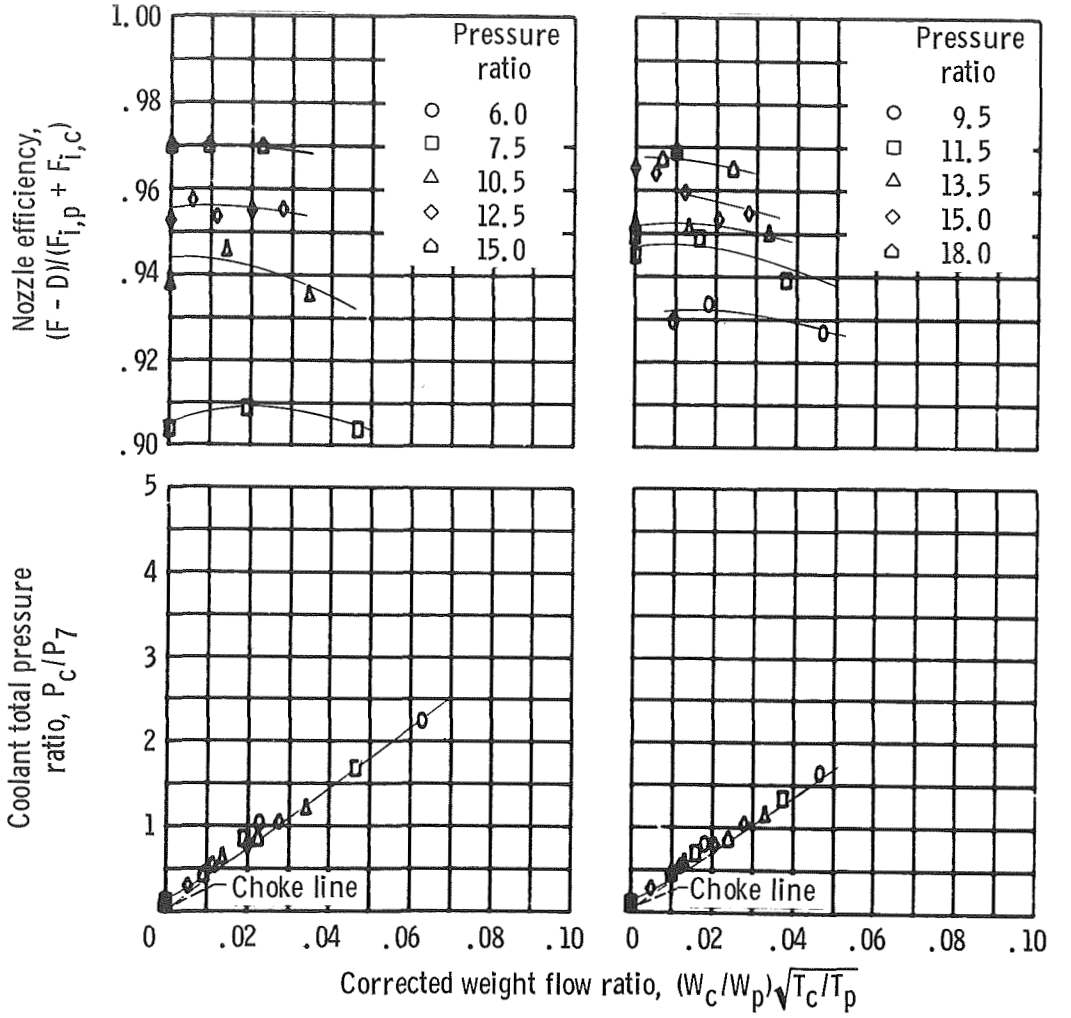

(j) Extended shroud; Mach number, 1.77.

(k) Extended shroud; Mach number, 1.97.

Figure 12. - Concluded.

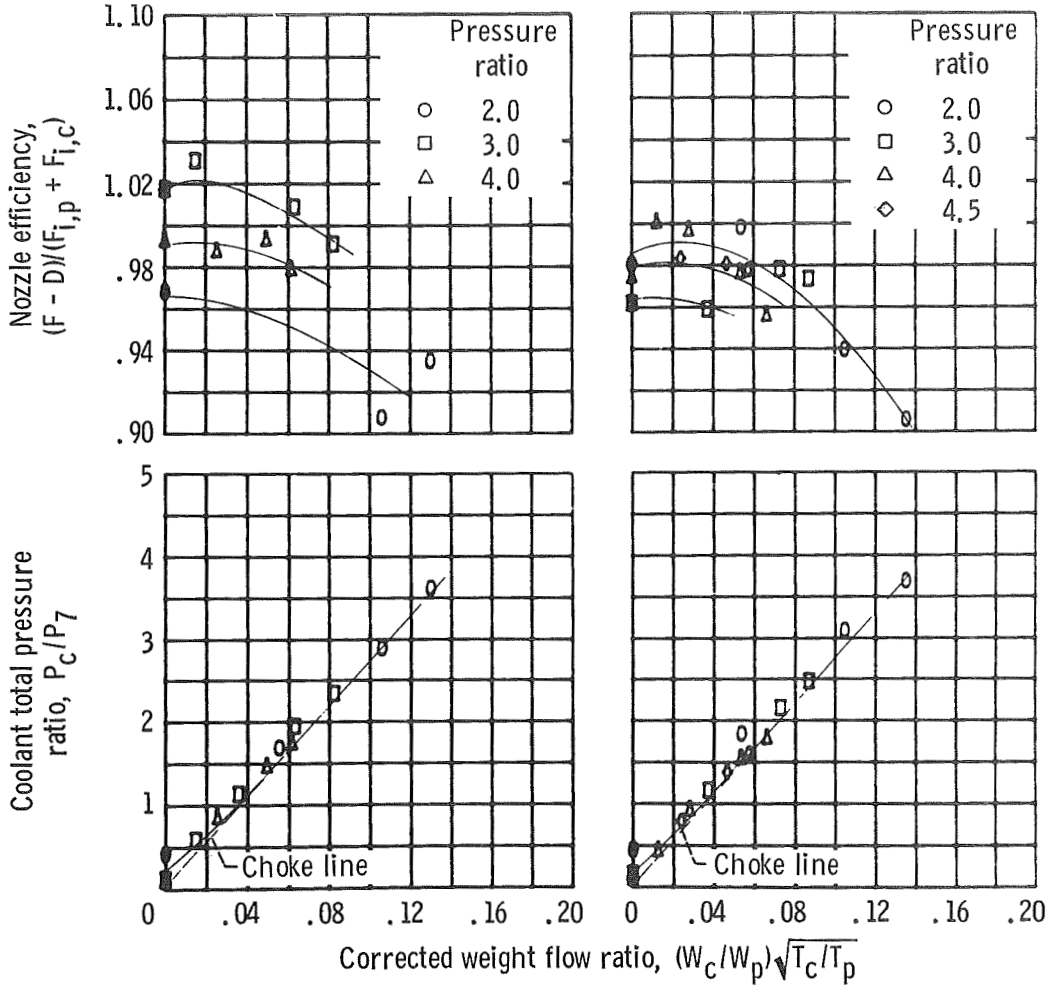

(a) Retracted shroud; Mach number, 0.

(b) Retracted shroud; Mach number, 0.6.

Figure 13. - Performance and pumping data. Full length plug; slot location x/l, 0.10; effective flow area ratio A_c/A_8, 0.034.

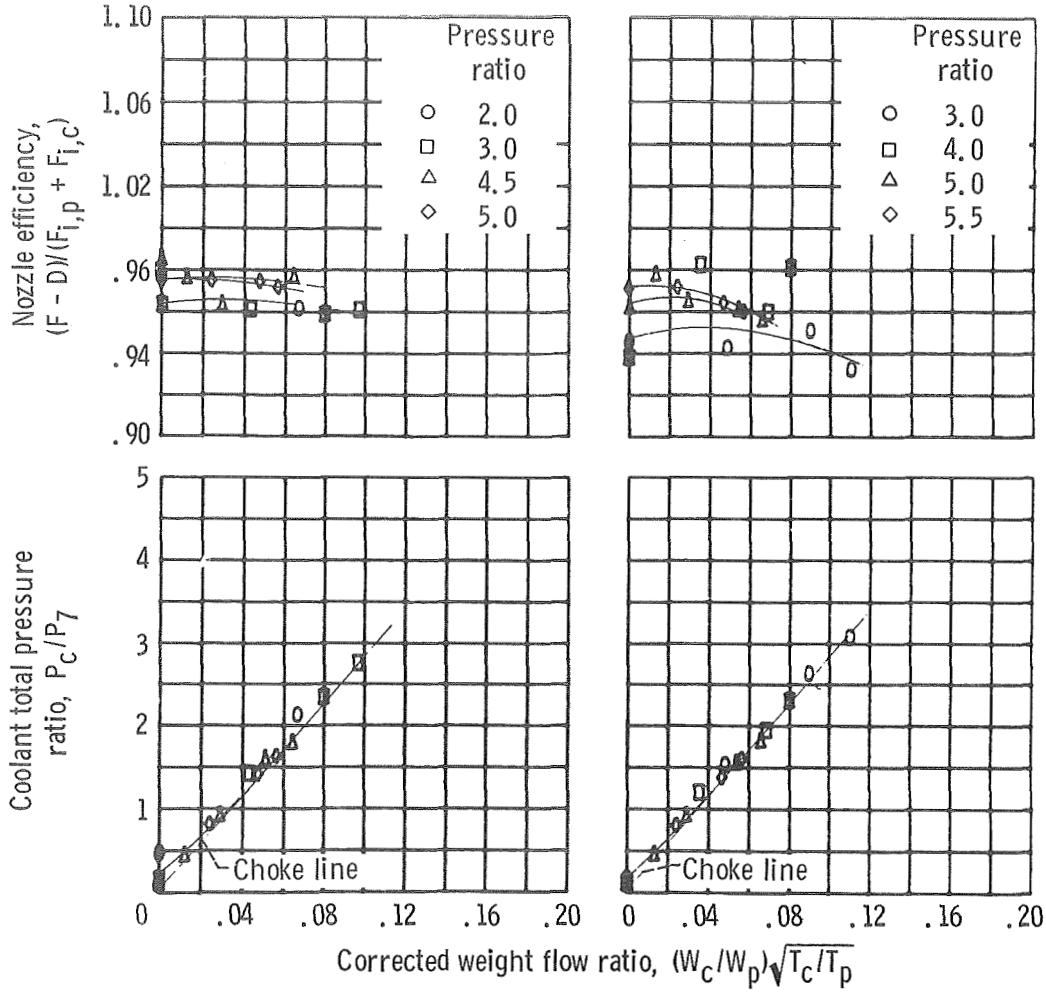

(c) Retracted shroud, Mach number, 0.7.

(d) Retracted shroud; Mach number, 0.8.

Figure 13. - Continued.

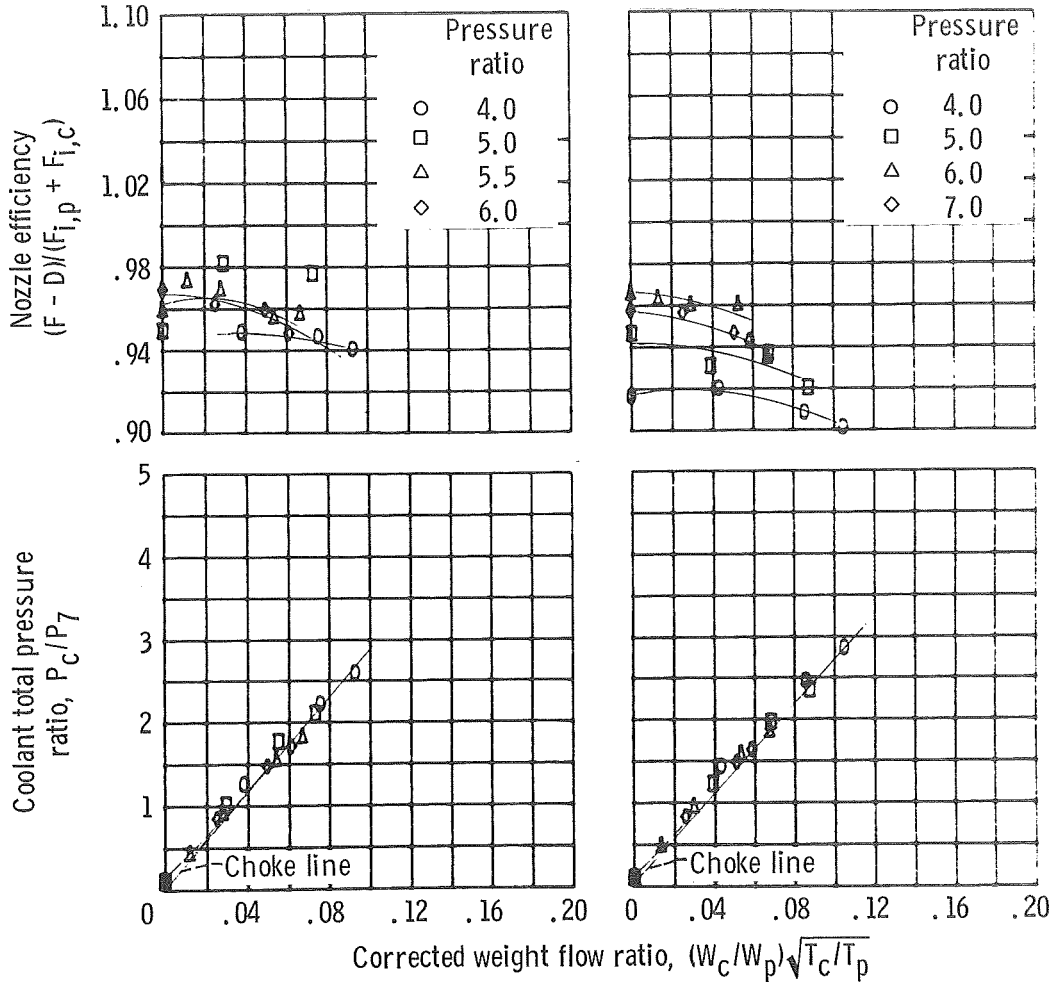

(e) Retracted shroud; Mach number, 0.9.

(f) Retracted shroud; Mach number, 1.0.

Figure 13. - Continued.

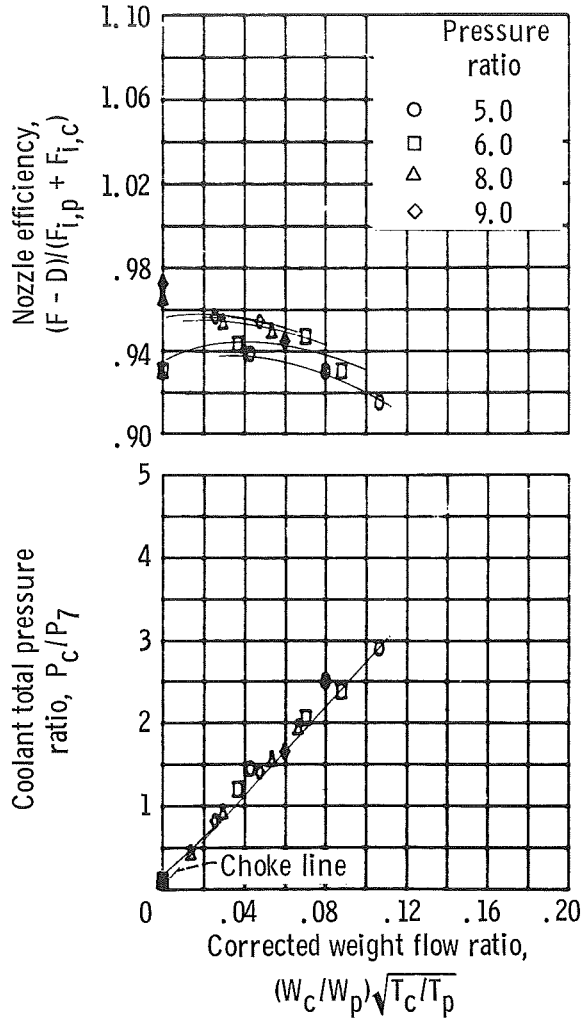

(g) Retracted shroud; Mach number, 1.2.

Figure 13. - Continued.

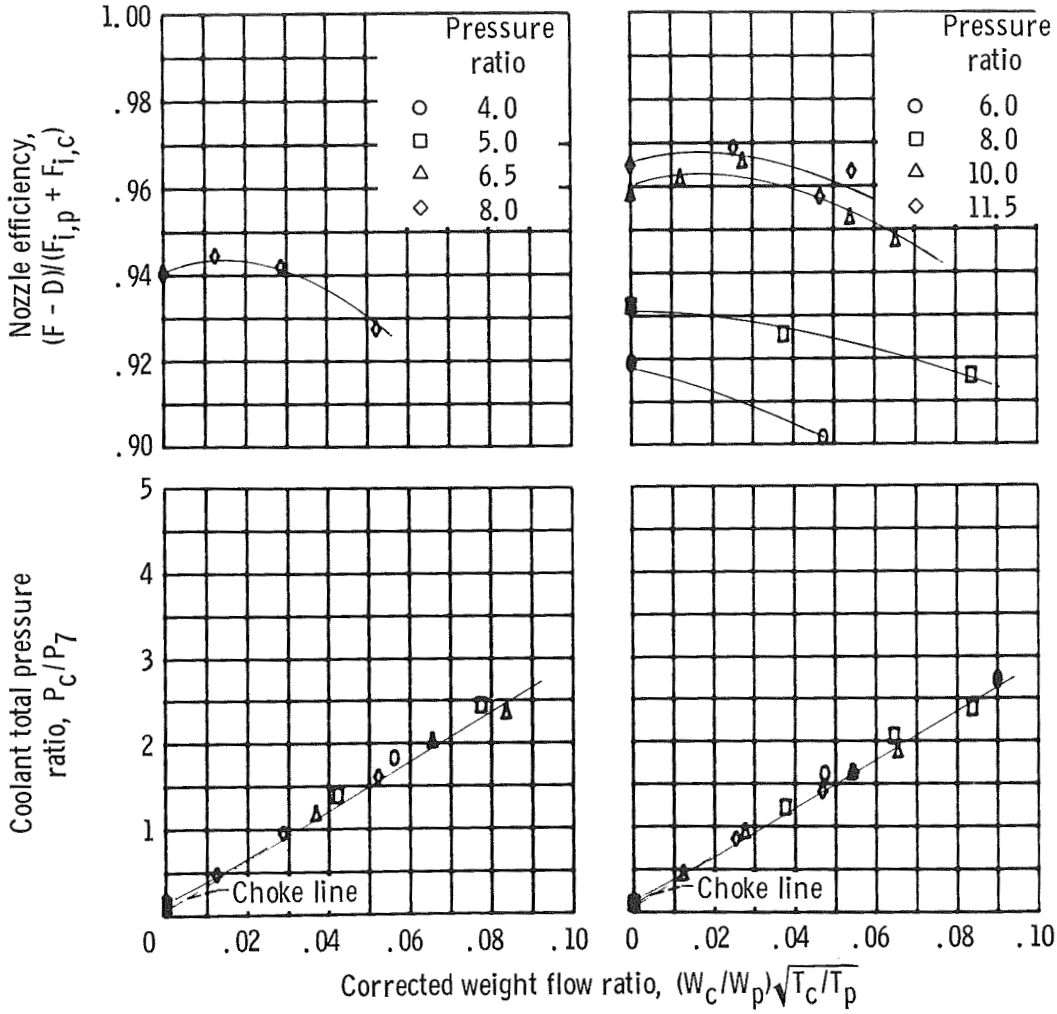

(h) Extended shroud; Mach number, 1.2.

(i) Extended shroud; Mach number, 1.47.

Figure 13. - Continued.

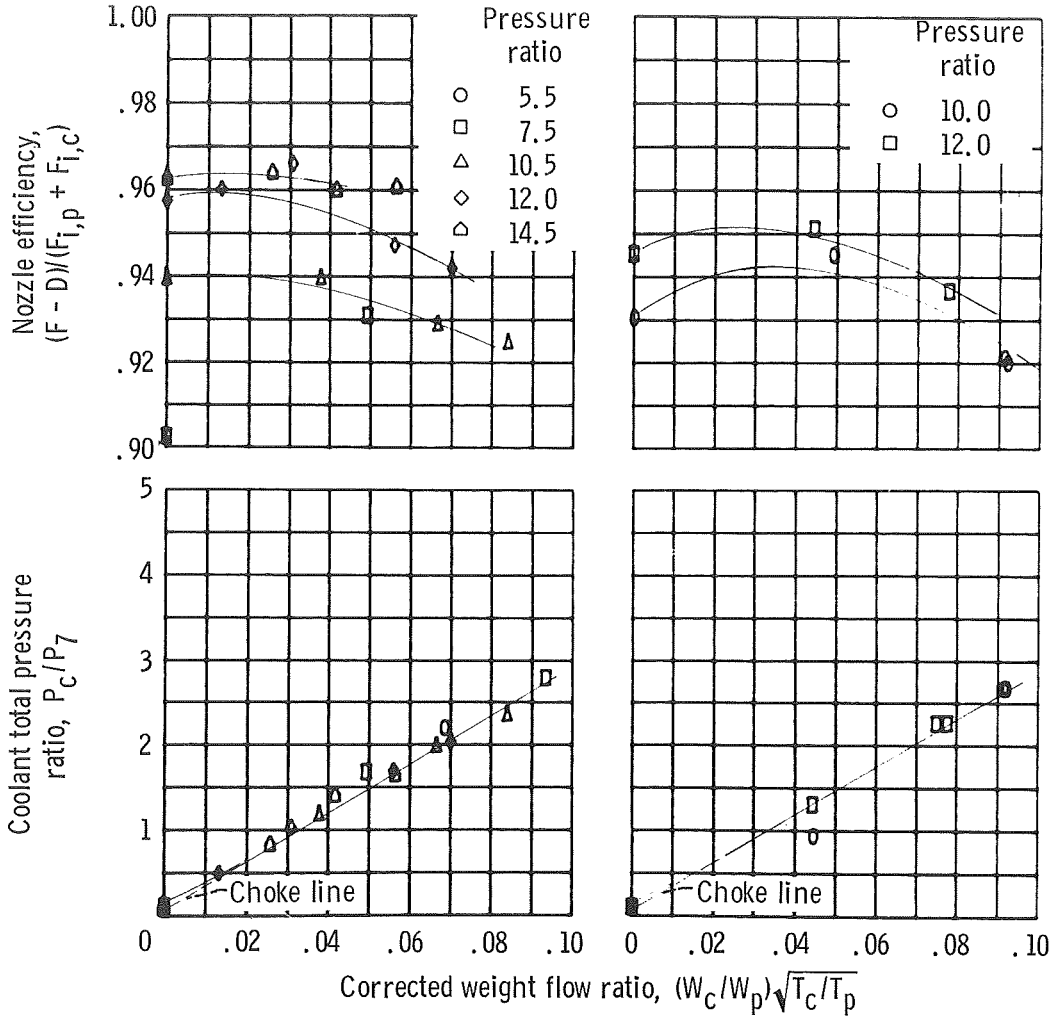

(j) Extended shroud; Mach number, 1.77.

(k) Extended shroud; Mach number, 1.97.

Figure 13. - Concluded.

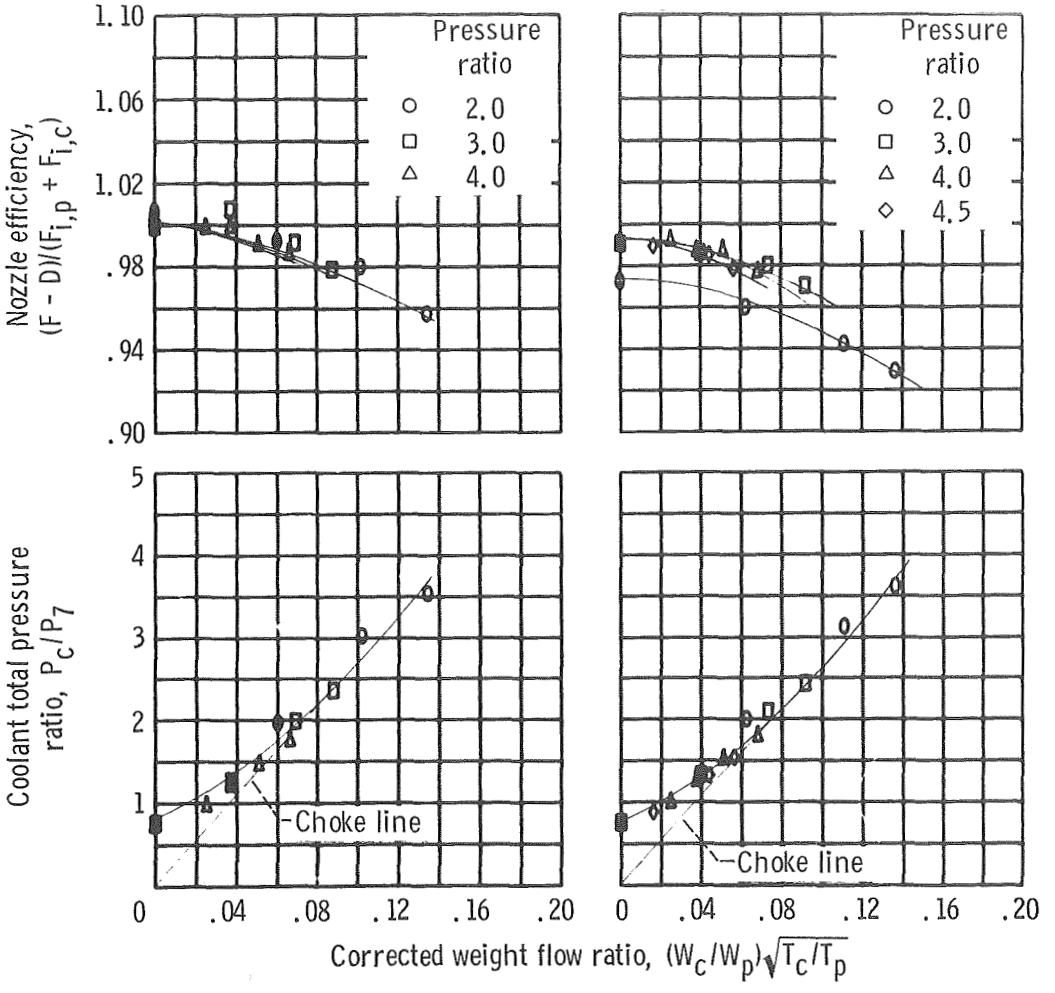

(a) Retracted shroud; Mach number, 0.

(b) Retracted shroud; Mach number, 0.6.

Figure 14. - Performance and pumping data. Full length plug; slot location x/l, -0.10; effective flow area ratio A_c/A_8, 0.039.

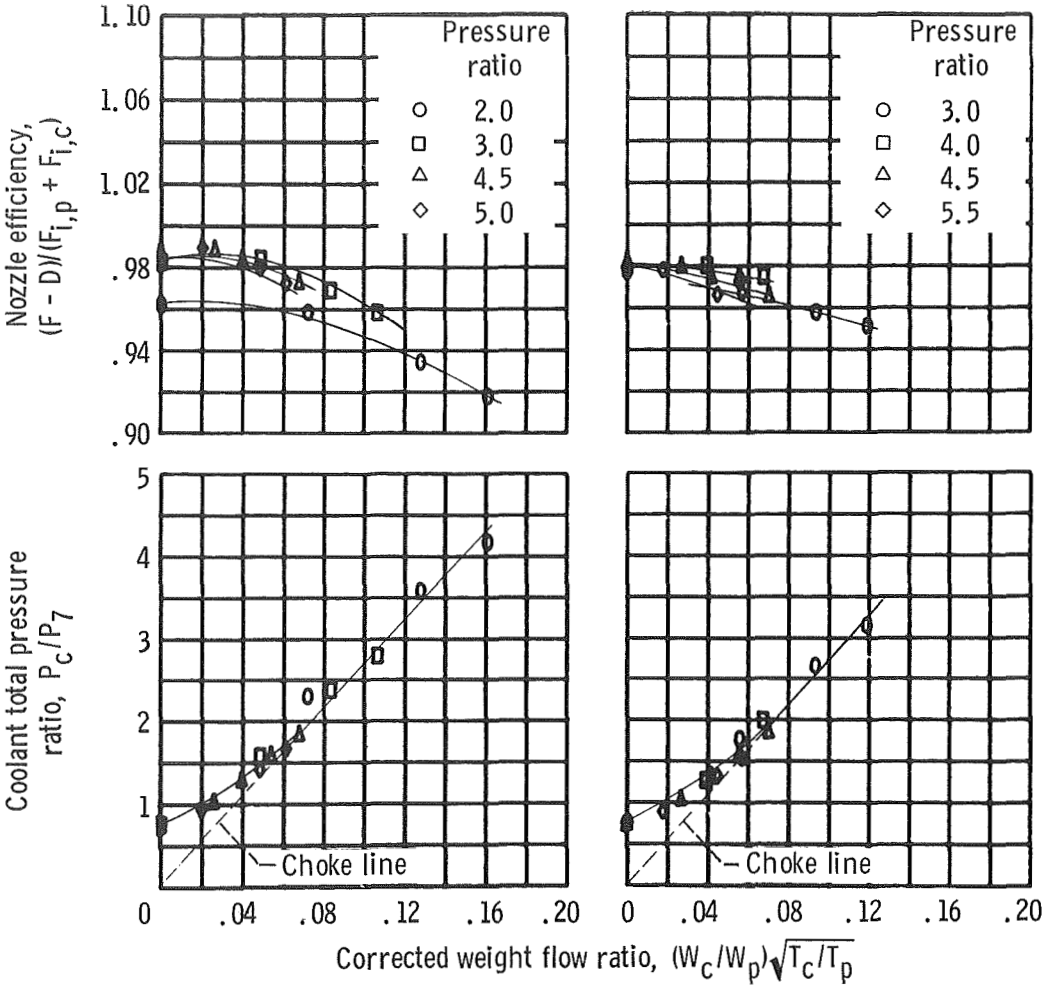

(c) Retracted shroud; Mach number, 0.7.

(d) Retracted shroud; Mach number, 0.8.

Figure 14. - Continued.

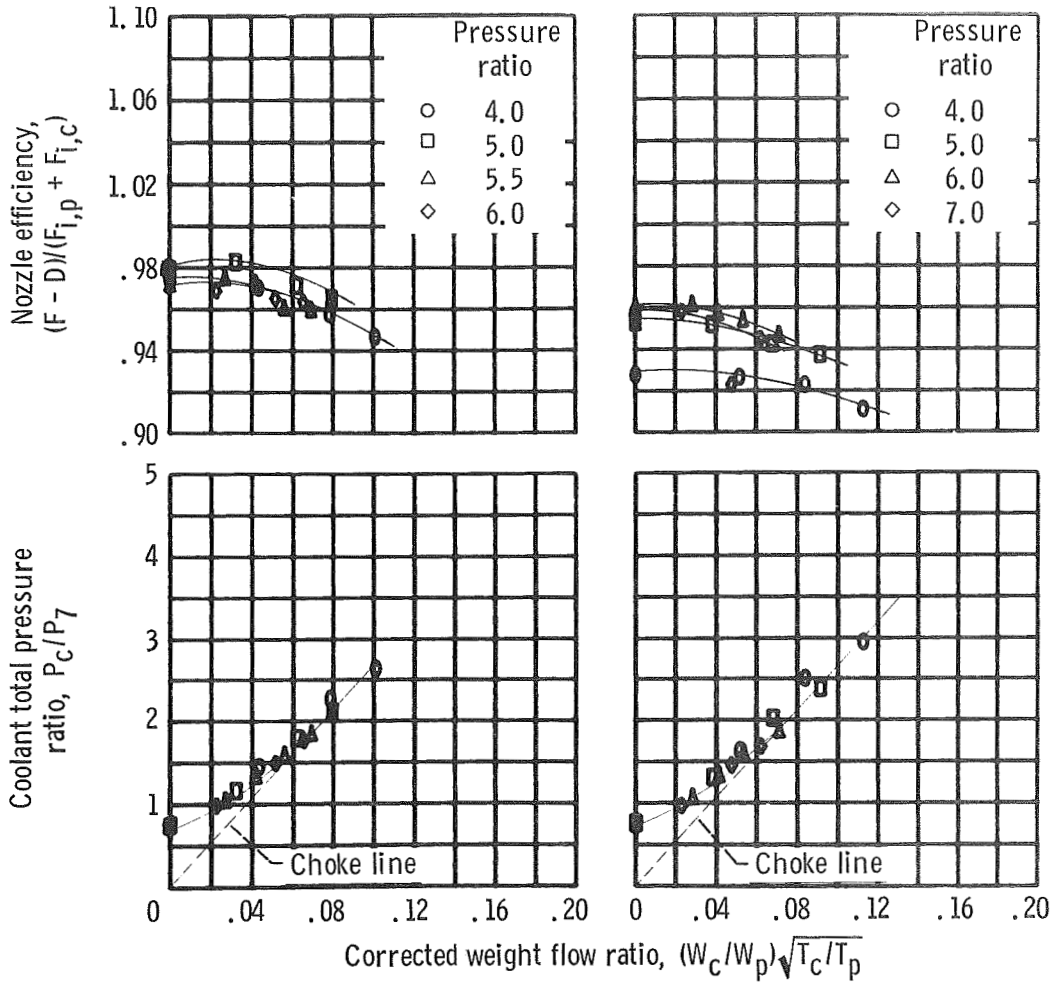

(e) Retracted shroud; Mach number, 0.9.

(f) Retracted shroud; Mach number, 1.0.

Figure 14. - Continued.

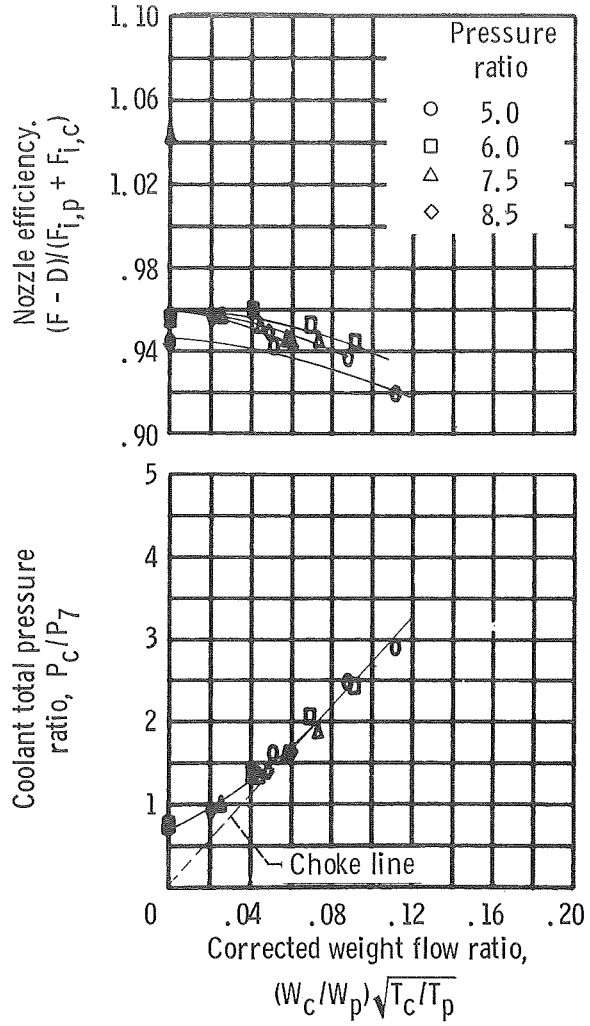

(g) Retracted shroud; Mach number, 1.2.

Figure 14. - Continued.

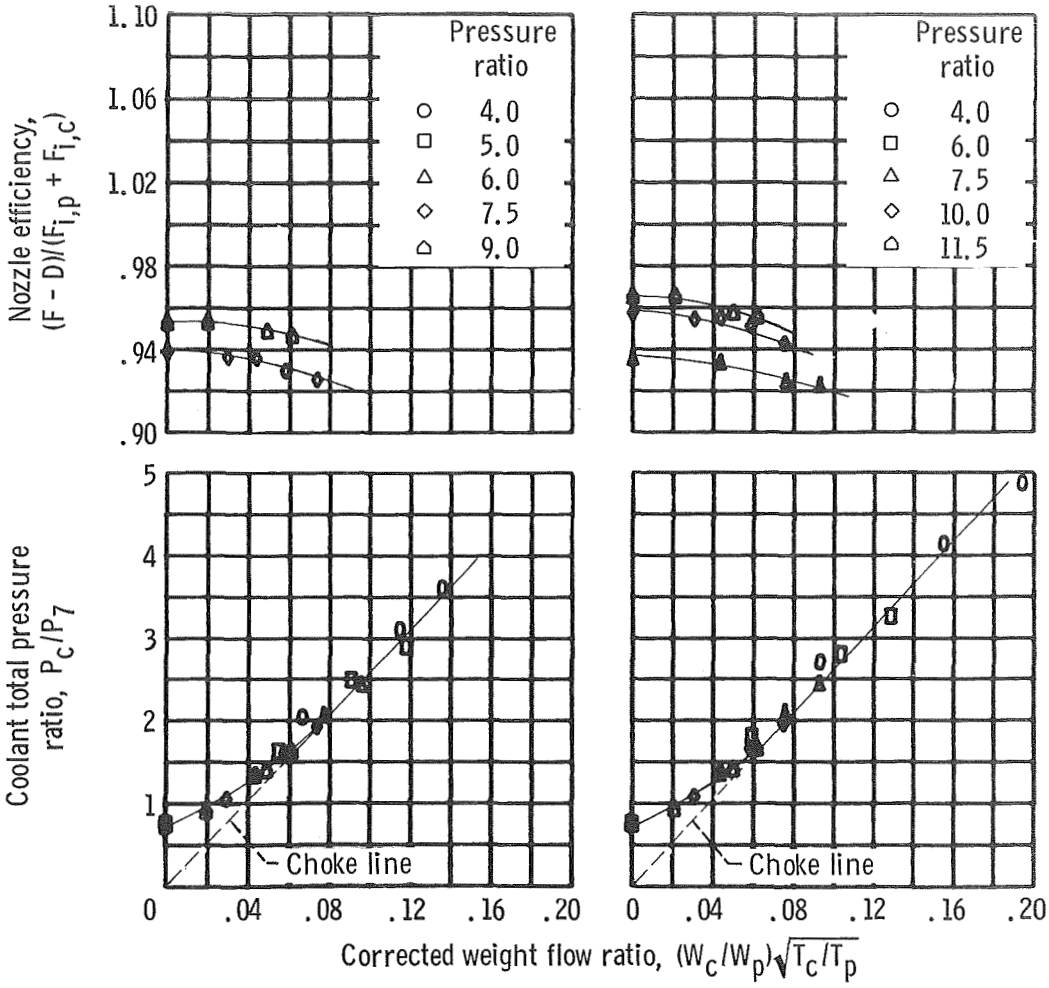

(h) Extended shroud; Mach number, 1.2.

(i) Extended shroud; Mach number, 1.47.

Figure 14. - Continued.

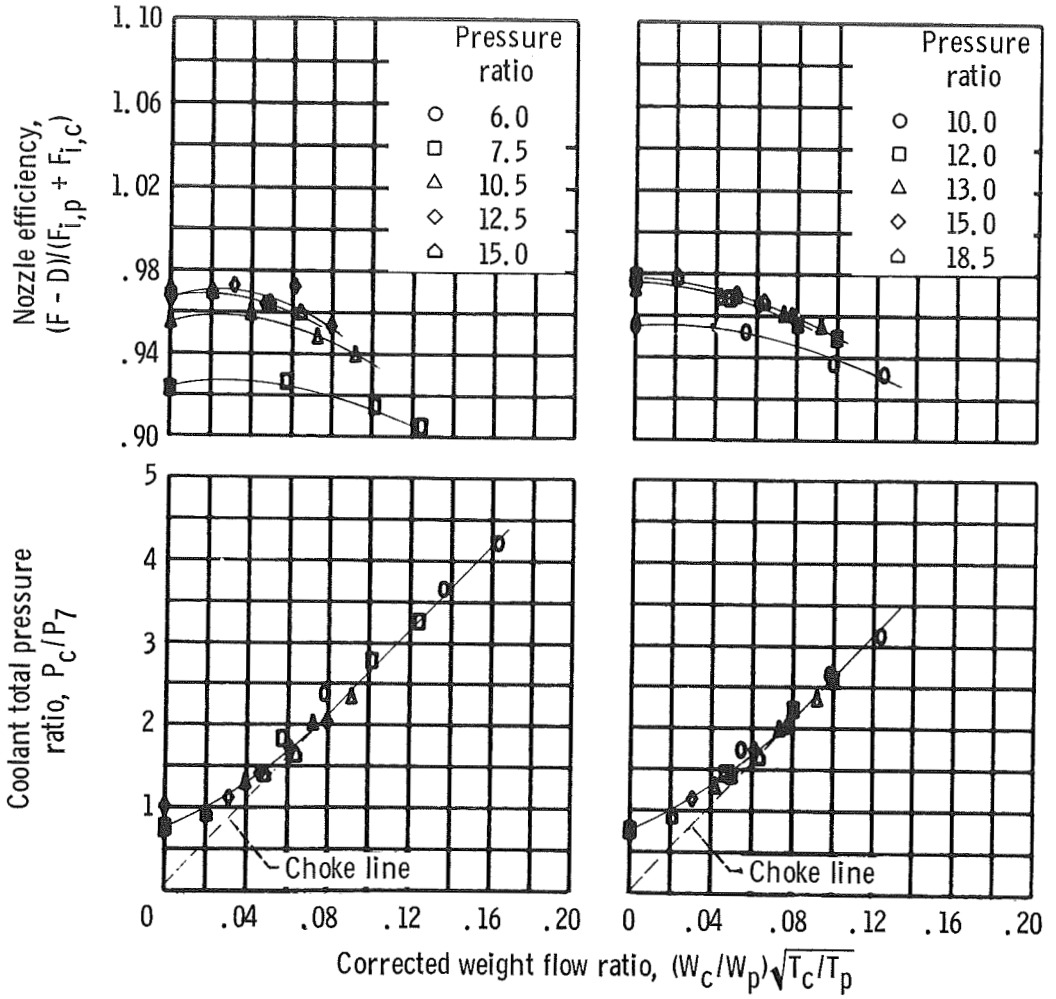

(j) Extended shroud; Mach number, 1.77.

(k) Extended shroud; Mach number, 1.97.

Figure 14. - Concluded.

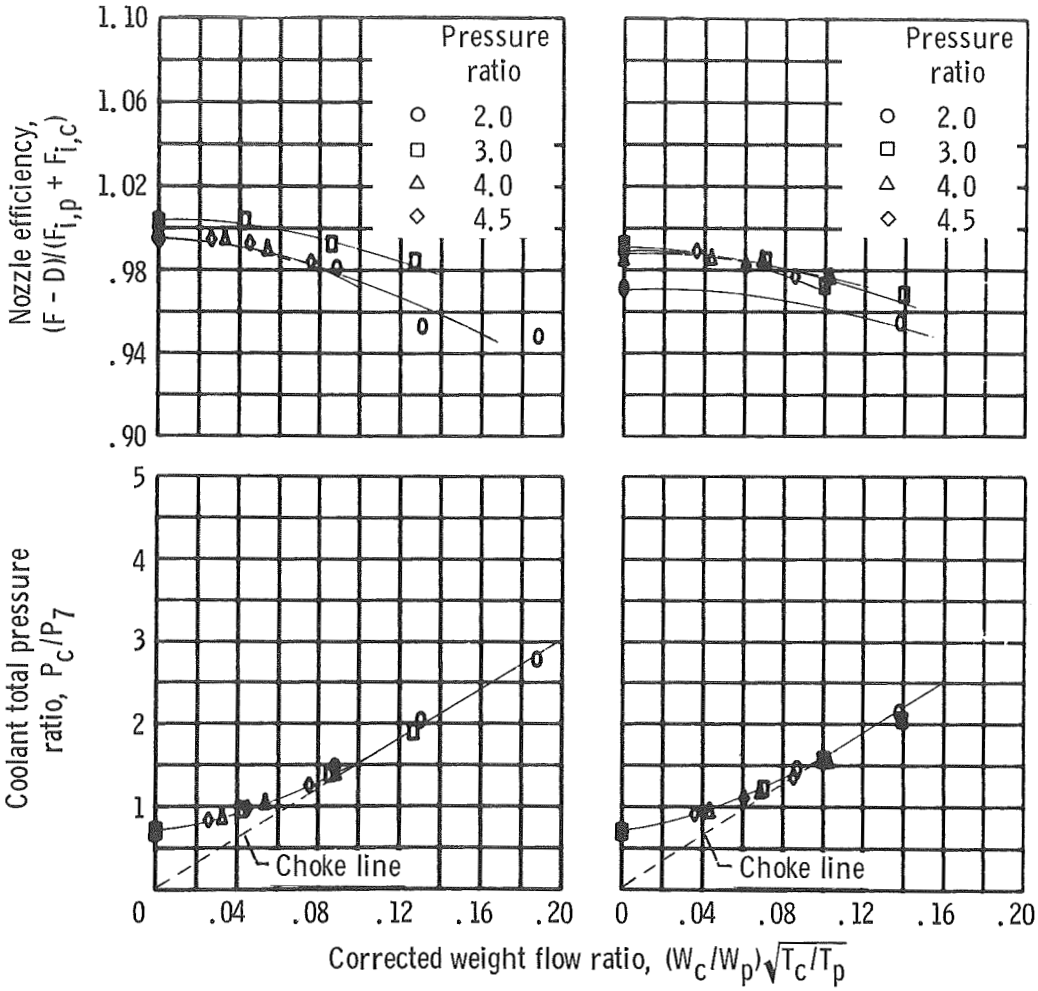

(a) Retracted shroud; Mach number, 0.

(b) Retracted shroud; Mach number, 0.6.

Figure 15. - Performance and pumping data. Full length plug; slot location x/l, -0.10; effective flow area ratio A_c/A_8, 0.067.

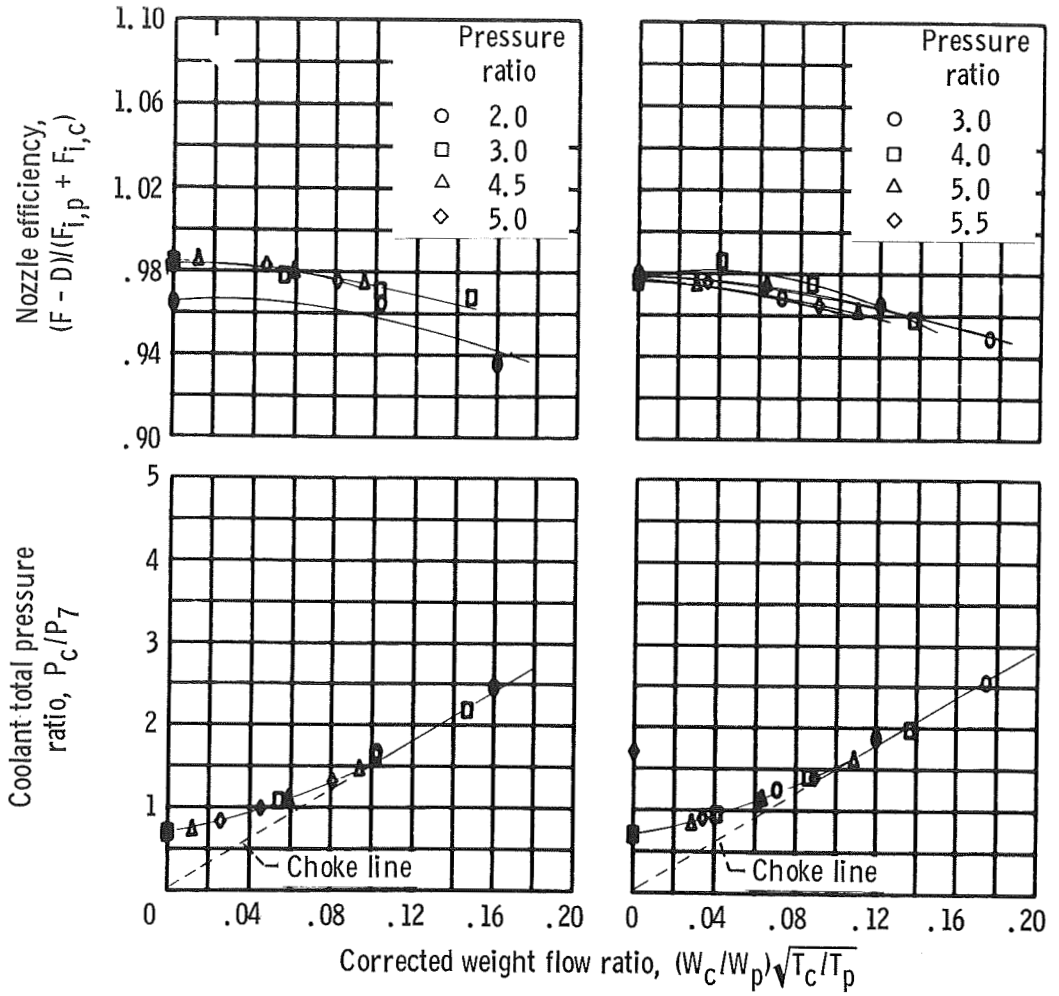

(c) Retracted shroud; Mach number, 0.7.

(d) Retracted shroud; Mach number, 0.8.

Figure 15. - Continued.

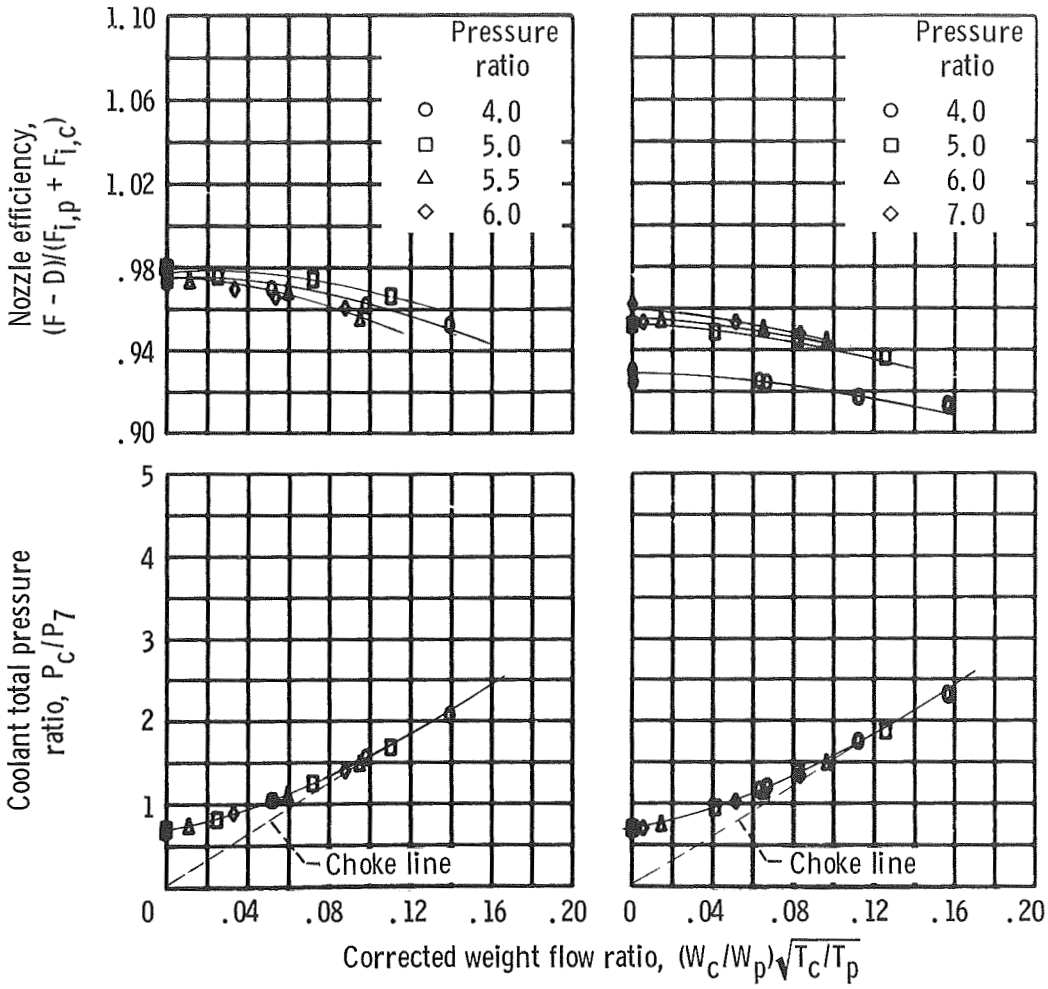

(e) Retracted shroud; Mach number, 0.9.

(f) Retracted shroud; Mach number, 1.0.

Figure 15. - Continued.

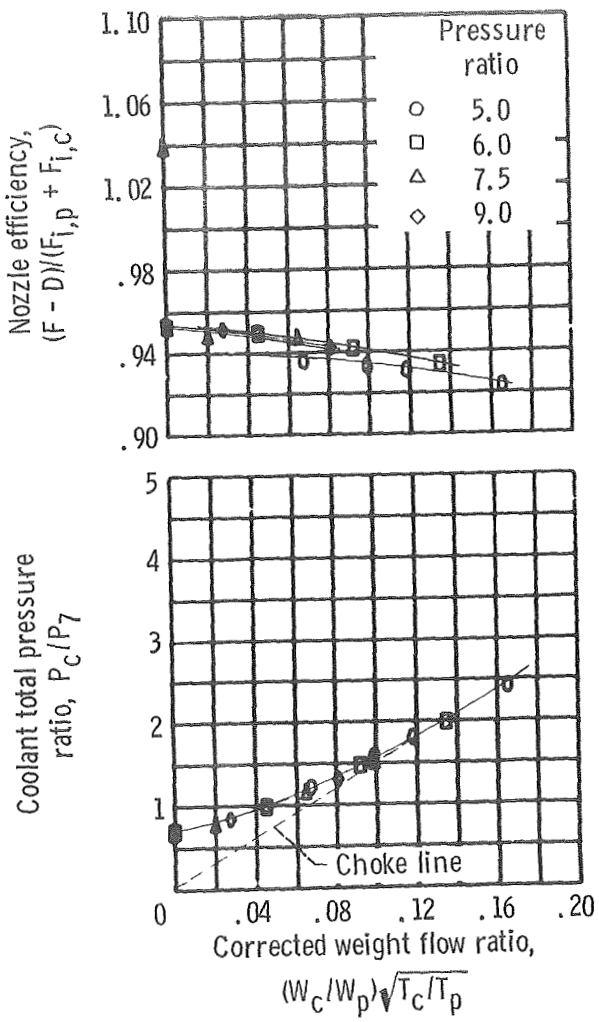

(g) Retracted shroud; Mach number, 1.2.

Figure 15. - Continued.

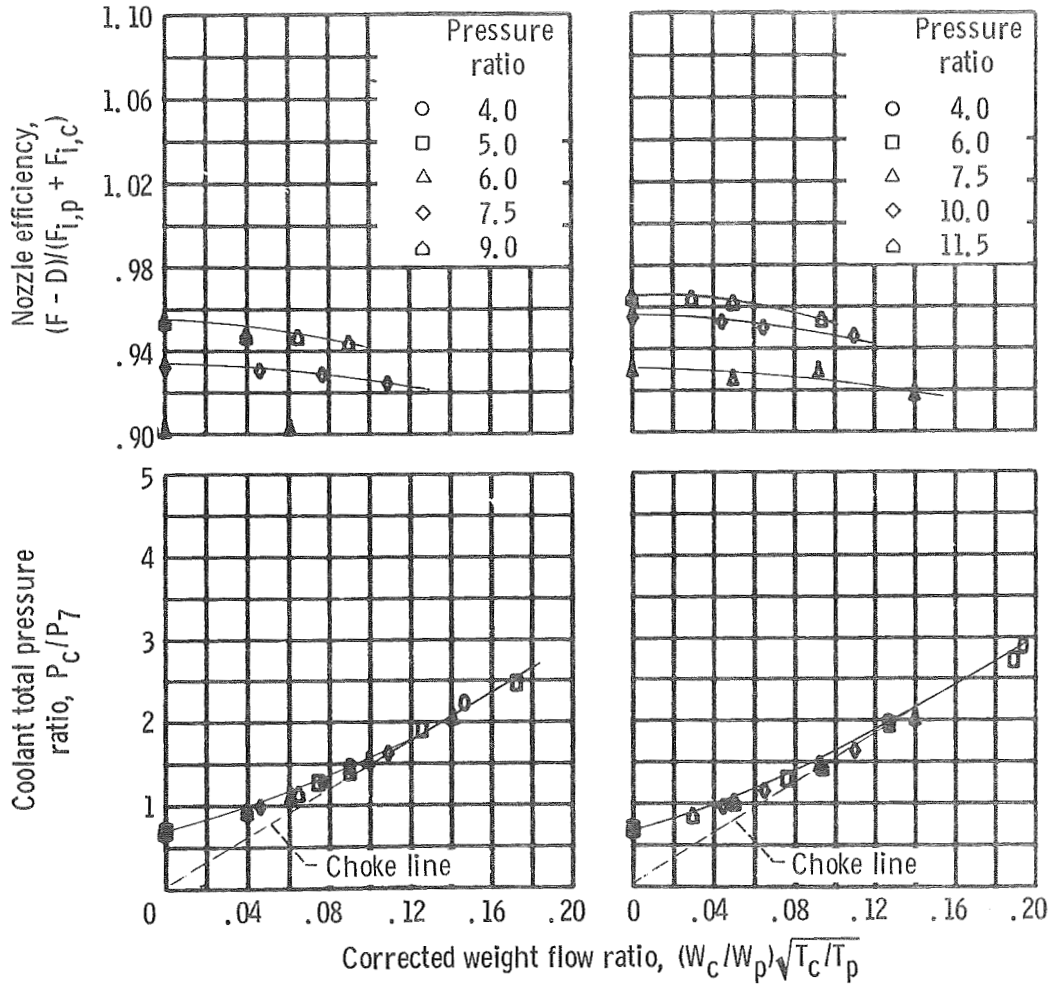

(h) Extended shroud; Mach number, 1.2.

(i) Extended shroud; Mach number, 1.47.

Figure 15. - Continued.

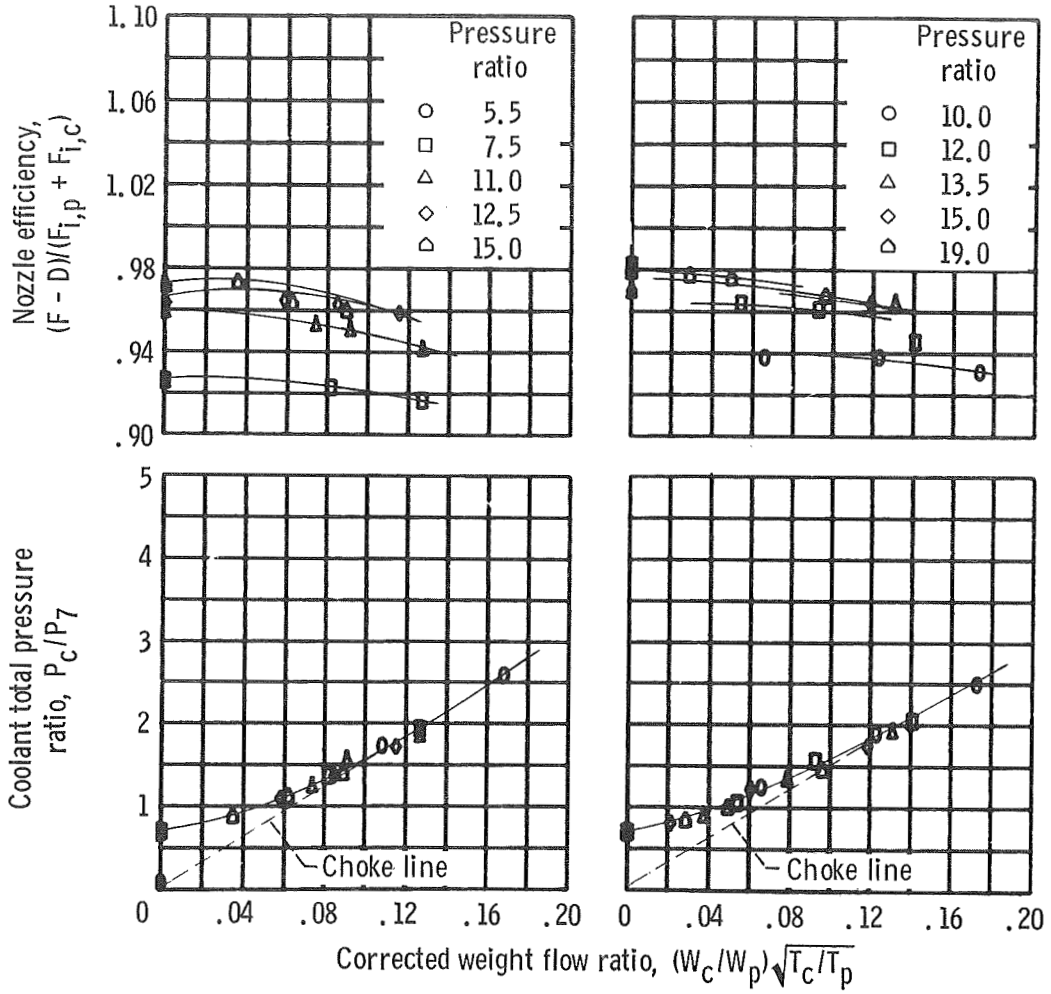

(j) Extended shroud; Mach number, 1.77.

(k) Extended shroud; Mach number, 1.97.

Figure 15. - Concluded.

REFERENCES

1. Bresnahan, Donald L.: Experimental Investigation of a 10^{o} Conical Turbojet Plug Nozzle with Iris Primary and Translating Shroud at Mach Numbers from 0 to 2.0. NASA TM X-1709, 1968.

2. Eckert, E. R. G.; and Livingood, John N. B.: Comparison of Effectiveness of Convection-, Transpiration-, and Film-Cooling Methods with Air as Coolant. NACA Rep. 1182, 1954.

3. Smith, K. G.: Methods and Charts for Estimating Skin Friction Drag in Wind Tunnel Tests with Zero Heat Transfer. Rep. ARC CP-824, Aeronautical Research Council, Great Britain, 1965. (Available from DDC as AD-487132.)

4. Harrington, Douglas E.: Jet Effects on Boattail Pressure Drag of Isolated Ejector Nozzles at Mach Numbers from 0.60 to 1.47. NASA TM X-1785, 1969.

NASA-Langley, 1970 —— 28 E-5552

"The aeronautical and space activities of the United States shall be conducted so as to contribute . . . to the expansion of human knowledge of phenomena in the atmosphere and space. The Administration shall provide for the widest practicable and appropriate dissemination of information concerning its activities and the results thereof."

—NATIONAL AERONAUTICS AND SPACE ACT OF 1958

NASA SCIENTIFIC AND TECHNICAL PUBLICATIONS

TECHNICAL REPORTS: Scientific and technical information considered important, complete, and a lasting contribution to existing knowledge.

TECHNICAL NOTES: Information less broad in scope but nevertheless of importance as a contribution to existing knowledge.

TECHNICAL MEMORANDUMS: Information receiving limited distribution because of preliminary data, security classification, or other reasons.

CONTRACTOR REPORTS: Scientific and technical information generated under a NASA contract or grant and considered an important contribution to existing knowledge.

TECHNICAL TRANSLATIONS: Information published in a foreign language considered to merit NASA distribution in English.

SPECIAL PUBLICATIONS: Information derived from or of value to NASA activities. Publications include conference proceedings, monographs, data compilations, handbooks, sourcebooks, and special bibliographies.

TECHNOLOGY UTILIZATION PUBLICATIONS: Information on technology used by NASA that may be of particular interest in commercial and other non-aerospace applications. Publications include Tech Briefs, Technology Utilization Reports and Notes, and Technology Surveys.

Details on the availability of these publications may be obtained from:

SCIENTIFIC AND TECHNICAL INFORMATION DIVISION

NATIONAL AERONAUTICS AND SPACE ADMINISTRATION

Washington, D.C. 20546